Analysis and Design of a Transistor Blocking Oscillator Including Inherent Nonlinearities

By J. A. NARUD and M. R. AARON

(Manuscript received July 17, 1958)

An analysis of transistor blocking oscillators is presented which differs significantly from previous approaches in that the nonlinear dependence of collector current and base voltage upon base current is considered. First, the nonlinear differential equations governing circuit performance are derived considering the effects of alpha cutoff, collector capacitance and leakage and magnetizing inductance. The relative importance of the various terms in this equation during transition, relaxation and recovery intervals is discussed from a physical viewpoint.

Analog and digital computer solutions of the nonlinear differential equation yield pulse responses which give excellent agreement with experimental results for various signals, transistor characteristics and values of passive circuit elements. The paper concludes with a design example in which the analysis is confirmed by experiment.

I. INTRODUCTION

Transistor blocking oscillators are finding application in digital computers[1] and transmission systems[2] where it is necessary to reconstruct a pulse train that has been dispersed in a noisy medium. In fact, several papers[3,4,5] have been published concerning the design and analysis of such circuits. All of the previous analytical approaches have been based on the use of a piecewise linear analysis. Linear circuit approximants have been used which are approximately valid during portions of the circuit operation, and formulas have been derived for the rise time and pulse width of the output pulse. The piecewise linear approach does not deal with the inherent nonlinear character of the circuit, and the approximations involved in linearization are often difficult to justify. The most serious shortcoming of the linearization technique is the fact that

it does not give information concerning trigger requirements for reliable operation.

In view of the inherent restrictions of the approximate analysis, a more detailed analysis which deals directly with the nonlinear nature of the circuit has been undertaken. The following sections of this paper will be concerned with the development of this procedure. First, the equivalent circuit, including the nonlinear dependencies, will be displayed and the assumptions on which the analysis is based will be discussed. The nonlinear integro-differential equations governing the performance of the circuit throughout its *entire cycle* of operation will be derived. A clear qualitative picture of the circuit operation is achieved with the nonlinearities included. Physical reasoning permits the dissection of the nonlinear equations into equations governing the circuit operation during the transition intervals ("off and on"), "on" interval and "recovery" interval. Trigger requirements for reliable regenerative action are derived. These are, of course, dependent on the nonlinear characteristics of the transistor as well as on other circuit parameters. Requirements on the circuit parameters to minimize ringing, achieve fast rise time, and recover quickly for repetitive operation are developed. Application of the results of the analysis to a specific example is given and confirmed by experiment.

Both analog and digital computers have been used as adjuncts to the strictly analytic approach to search out relationships between circuit parameters to achieve desired performance. It is believed that the combined analytical and computer approach used in this paper is more general and more easily applied than the piecewise linear analysis and, furthermore, that it is a valuable design philosophy for exploring other nonlinear circuits. Further work on other nonlinear transistor circuits using this approach is being pursued.

II. THE EQUIVALENT CIRCUIT

In selecting the equivalent circuit for an active device one is usually confronted with two conflicting requirements. On the one hand, the equivalent circuit must accurately exhibit the same properties as the physical device, so that computations based on the equivalent circuit give substantial agreement with experiment. On the other hand, there is a twofold requirement for simplicity. First, the number of parameters involved should be minimized to make the analysis tractable. Second, it should be possible to draw qualitative conclusions regarding the circuit operations from the equivalent circuit. In the case of the transistor blocking oscillator, these requirements are particularly important. Since the oscillator is highly nonlinear in its operation the number of coupled

equations involved is closely related to the complexity of the equivalent circuit.

With these factors in mind, the equivalent circuit shown in Fig. 1(a) was chosen to represent the transistor in the grounded emitter blocking oscillator. It takes into account the following properties of the transistor: (a) the nonlinear relationship between base voltage and base current; (b) the nonlinear dependence of collector current on base current and frequency; (c) partially, the effect of minority carrier storage during "turnoff" and (d) the combined effect of collector and stray capacitance.

However, the circuit neglects, among other things, the effect of coupling between the base and the collector circuit, emitter junction capacitance, base spread resistance and recombination. In the following we will discuss the quantities listed above, and how they can be obtained from measurements on the transistor. The surface barrier transistor 2N128 will be used throughout this paper to exemplify the procedure; the results are applicable to other types of junction transistors with broadly similar characteristics. Modifications in the analysis to accommodate drastic differences from this model can be made, with an attendant increase in the complexity of the analysis.

2.1 *Nonlinear Relationship Between Base Voltage and Base Current*

In the equivalent circuit of Fig. 1(a) the nonlinear relationship between base voltage and current is denoted by;

$$v_b = V_b(i_b). \tag{1}$$

The dependence on collector current has been neglected since, as shown later, the terms involving v_b in the equations governing the blocking oscillator are negligible during the "turn-on" and "on" intervals. Thus, v_b may be obtained by measuring the base voltage as a function of base current, with the collector circuit connected to the load and bias with which it will normally operate. The result of such a measurement is shown in Fig. 1(b). It is seen that this result is almost a straight line above a certain value of i_b (saturation) and almost vertically straight when $i_b < 0$. Thus, it can sometimes be approximated by two straight-line segments through the origin with different slopes.[5] Another way of approximating it is to use the relationship between current and voltage of p-n junction diodes:[6]

$$I = I_s(e^{qV/kT} - 1), \tag{2}$$

where $kT/q = 0.026$ volt at room temperature (25°C) and I_s is the reverse saturation current.

2.2 *Nonlinear Dependence of Collector Current on Base Current and Frequency*

The dependence of the collector current upon base current and frequency is assumed in the equivalent circuit to be of the form

$$\left(1 + \frac{1}{\omega_0}\frac{d}{dt}\right) i_c = I_c(i_b), \tag{3}$$

where $I_c(i_b)$ represents the static collector-current-base-current characteristic, i_c the actual collector current, and ω_0 the "large-signal" cutoff frequency or inverse time constant of the transistor. This expression is the "large-signal" equivalent of the linear relationship

$$\beta(s) = \frac{\beta_0}{1 + \dfrac{s}{\omega_\alpha(1 - \alpha_0)}} = \frac{\dfrac{dI_c}{di_b}}{1 + \dfrac{s}{\omega_\alpha(1 - \alpha_0)}}. \tag{4}$$

The derivative of (3) with respect to i_b reduces to (4) when the circuit operation is linear. The function $I_c(i_b)$ may be determined experi-

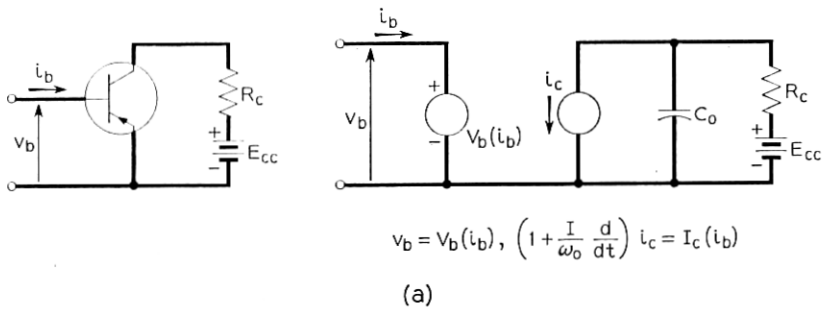

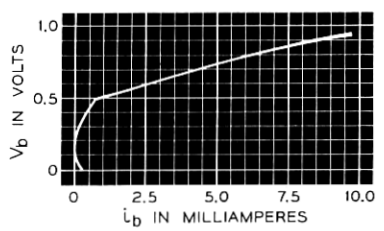

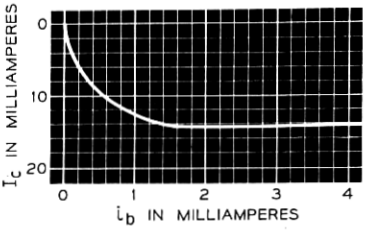

Fig. 1 — (a) The grounded emitter configuration and its large-signal equivalent circuit: (b) v_b vs. i_b ; (c) i_c vs. i_b .

TABLE I

2N128 Unit No.	I_{bs}, ma	I_{cs}, ma	$\bar{\beta}$	f_α, mc	f_0, mc	Rise Time with 100-ohm Load, mμs		Fall Time, Measured, mμs	f_{0t} Fall, mc	$C_c(V_{cc})$, μμf	T_R observed / T_R computed, 400-ohm Load
						Calculated	Measured				
92	2.25	14	6.22	106.5	14.75	23.8	21	145	2.41	2.3	0.85
150	2.0	14	7.0	66.5	8.32	42.1	46	240	1.46	1.6	1.2
151	1.0	14	14.0	120	8.0	43.8	42	190	1.84	1.6	1.06
176	1.88	14	7.45	63.3	7.5	47	53	260	1.35	2.1	1.15
273	1.25	14	11.2	99	8.1	43.2	39	140	2.50	3.0	0.94
369	1.63	14	8.59	36	3.75	93.4	88	260	1.35	3.0	0.87
Average Values						48.8	48.2				1.01

mentally by measuring the collector direct current for various values of base current, with the collector connected to the load and bias with which it will normally operate. Such a characteristic is shown in Fig. 1(c). It is seen that $I_c(i_b)$ saturates very sharply, the saturation value being approximately E_{cc}/R_c. In some cases in the subsequent analysis it will be convenient to approximate this function with an analytic expression.

From (4) it is seen that, when the circuit operation is linear, the effective cutoff frequency, ω_0, for the grounded emitter configuration is

$$\omega_0 = \omega_\alpha(1 - a) = \frac{\omega_\alpha}{1 + \beta}, \tag{5}$$

and therefore is dependent upon ω_α and β. Thus, as the operating point is changed, ω_0 will vary, having a minimum when β (or α) is a maximum and becoming equal to ω_α when $\beta = 0$ as, for example, at cutoff or saturation. When a large signal is applied to the transistor, ω_0 will, therefore, change continuously as the various points of the i_c/i_b characteristics are traversed and the "effective cutoff frequency" will then be some kind of average of (5). Although ω_α is also dependent on the location of the operating point,[7] it has been found that the ω_α determined at standard bias (V_{cc}) yields transient results which agree closely with experiment. These results are shown in Table I and discussed further below.

Moll[8] has suggested the following calculation of the large-signal cutoff frequency, ω_0: If an average β is defined as the ratio of the total excursion of the collector and base currents; that is,

$$\bar{\beta} = \frac{I_{c\,\max} - I_{c\,\min}}{I_{b\,\max} - I_{b\,\min}}, \tag{6}$$

then the large-signal cutoff frequency is given by:

$$\omega_0 \doteq \frac{\omega_\alpha}{1 + \bar{\beta}}. \tag{7}$$

Accordingly, in a circuit like the blocking oscillator, in which the operation extends from cutoff to saturation, ω_0 will be given by (neglecting I_{co})

$$\omega_0 \doteq \frac{\omega_\alpha}{1 + \dfrac{I_{cs}}{I_{bs} - I_{bc}}}. \tag{8}$$

The large-signal cutoff frequency may also be determined experimentally by applying a current step function of magnitude I_{bs} to the base and then measuring the 10 to 90 per cent rise time of the voltage across the load resistance. Since the output response can be described by a single exponential, provided the load resistance, R_c, is selected to be so small that the effect of the collector capacitance may be neglected, ω_0 is given by:

$$\omega_0 \doteq \frac{2.2}{T_R}, \tag{9}$$

where T_R is the 10 to 90 per cent rise time. In Fig. 2(a) the output response is shown for steps of various magnitudes in base current. It is seen that the rise time continually decreases as the size of the step increases, and that the response is very nearly exponential in shape, thereby justifying the above approximation.

With two ways of calculating ω_0, the natural question that arises is how well these two methods agree. To provide a partial answer to this question, the calculated and measured rise times of six transistors were compared. The rise time was computed by use of (8) and (9) and measured across a 100-ohm load when a current step function of magnitude I_{bs} was applied to the base. The results are shown in Table I, from which it is seen that the calculated and measured values agree within ± 10 per cent and the average values agree within 2 per cent. Taking into account the error involved in measuring rise times from the face of an oscilloscope, the agreement is indeed quite good.

2.3 *Effect of Minority Carrier Storage During Turnoff*

The effect of minority carrier storage in the collector-base region is not very easily related to any of the commonly measured transistor parame-

ters. The most convenient way to take it into account is to determine its effective time-constant experimentally. Fig. 2(b) shows the voltage across a 400-ohm load resistor in series with the collector of a junction surface barrier transistor (2N128) when various square current pulses are applied to the base. The rise time, fall time and width of the applied current pulse were 1, 7 and 100 milimicroseconds, respectively, and its magnitude was varied in steps from 0.2 to 10 ma. The base saturation current for that particular transistor (Unit 151) was 1 ma. From the

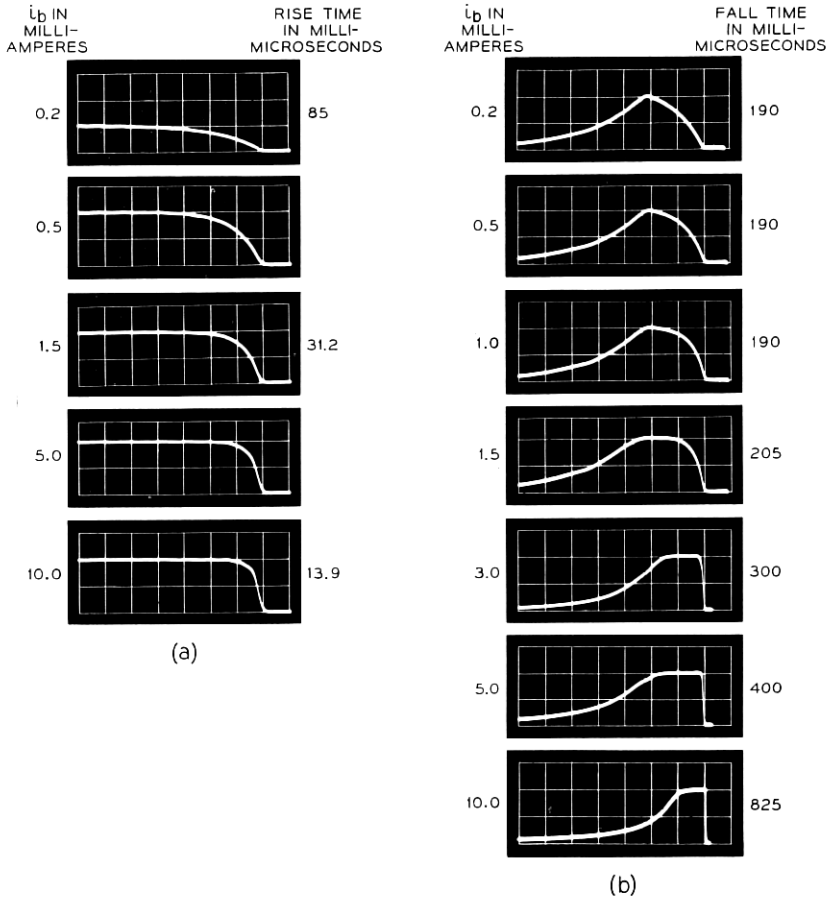

Fig. 2 — Collector current in response to (a) a step of base current, i_b ; (b) a pulse in base current of magnitude i_b , with rise time of 1 mμ sec, fall time of 7 mμ sec and width of 100 mμ sec. Time scales: (a) 25 mμ sec/division; (b) first four curves, 50 mμ sec/division; next two curves, 100 mμ sec/division; bottom curve, 250 mμ sec/division.

figures it is seen that, in contrast to the rising edge of the output pulse, the falling part becomes slower as the magnitude of the input pulse is increased. Also, the 10 to 90 per cent fall time is almost constant up to saturation, after which it increases rapidly. Again, since the falling response has roughly an exponential shape the fall time can be used to estimate the equivalent ω_0 during turnoff by the relationship:

$$\omega_{01} \sim \frac{2.2}{T_f}. \tag{10}$$

Columns 8 and 9 of Table I list the fall times and the corresponding ω_{01}'s for the six transistors.

2.4 *Combined Effect of Collector and Stray Capacitance*

In the small-signal case the output impedance of the grounded emitter configuration is:

$$Z_0 = Z_c(1 - \alpha) + r_e \frac{r_b + \alpha Z_c + Z_g}{r_b + r_e + Z_g}, \tag{11}$$

where Z_g is the impedance of the generator driving it. Since, in the blocking oscillator, Z_g is large and r_e is very small, the output impedance consists essentially of a capacitance of magnitude

$$C_0 = \frac{C_c}{1 - \alpha} = C_c(1 + \beta). \tag{12}$$

Under large-signal operation, both β and C_c will vary over the range, the collector capacitance varying with the collector voltage as

$$C_c = kV^{-r}, \tag{13}$$

where the exponent r is $\frac{1}{2}$ for step junctions and $\frac{1}{3}$ for uniformly graded junctions. Measurements made on a dozen 2N128 transistors yield an average value for r very close to $\frac{1}{3}$.

Bashkow[9] has shown that, as far as transient analysis is concerned, this nonlinear capacitance may be replaced by an average capacity C_{av}. The average capacity is defined as that which displaces the same charge as the nonlinear capacity for the same voltage change. A minor generalization of Bashkow's results yields

$$C_{av} = \frac{C_c(V_{cc})}{1 - r} \frac{1 - \left(\frac{V_1}{V_{cc}}\right)^{1-r}}{1 - \frac{V_1}{V_{cc}}}, \tag{14}$$

where V_{cc} is the collector voltage at cutoff and V_1/V_{cc} is the ratio of the

voltage swing on the collector. For a swing from V_{cc} to 0, and $r = \frac{1}{3}$, (12) becomes

$$C_0 = 1.5C_c(1 + \bar{\beta}), \tag{15}$$

where, as in the case of ω_0, β has been replaced by $\bar{\beta}$. In a physical circuit, stray capacity from collector to ground should be added to C_0.

With the transistor characterized in this manner it is readily shown that the Laplace transform of the collector current of the resistively loaded (R_c) common emitter stage is given by

$$I_c(s) = \frac{I_{cs}}{s\left(\frac{s}{\omega_0} + 1\right)(R_cC_0s + 1)} \tag{16}$$

for a step function in base current sufficient to saturate the transistor. To check the validity of the equivalent circuit, the 10 to 90 per cent rise time was computed for six transistors from the inverse transform of (16), using (7) and (15).* The rise time was also determined experimentally and the ratio of observed rise time to computed rise time is given in the last column of Table I. It can be seen that agreement within ± 15 per cent has been achieved on individual units, and that the average is within 2 per cent. These figures are within both the experimental error in reading a scope face and the error inherent in determining C_c, ω_α and $\bar{\beta}$.

In passing, it should be noted that a good approximation to the 10 to 90 per cent rise time is given by

$$T_R = \frac{2.2}{\omega_0}\sqrt{1 + \omega_0^2R_c^2C_0^2}. \tag{17}$$

The above expression results from (16) by an application of the rise time definition given by Elmore.[10] This will be mentioned again in the section devoted to the rise time of the blocking oscillator. It can also be shown by using Elmore's expression that the delay time (time to traverse from zero to 50 per cent of the final output) is given by

$$T_0 = \frac{1 + \omega_0R_cC_0}{\omega_0}. \tag{18}$$

Over a wide range of parameters, two times the time delay, as given above, is a very close approximation to the actual rise time. In this case, the rise time [two times (18)] is similar in form to that given by Easley[7] and can be justified by other considerations.[11]† Equation (18) will be

* 5 micromicrofarads were added to C_0 to account for stray socket and wiring capacity.

† Several definitions of rise time are given in Ref. 11, one of which, when applied to the grounded emitter stage, yields (18).

useful in the following sections in indicating how the factors in the design of the transistor blocking oscillator can be related to the rise time or delay time of the resistively loaded transistor alone.

Before proceeding to the blocking oscillator, it should be mentioned that the equivalent circuit of Fig. 1(a) may be used for the grounded base configuration. In this case, $\omega_0 = \omega_\alpha$ and $C_0 = 1.5C_c$. Therefore, the following discussion is also applicable to the grounded-base case.

III. THE GROUNDED EMITTER TRANSISTOR BLOCKING OSCILLATOR

Fig. 3 shows the circuit diagram as well as the equivalent circuit for the grounded emitter blocking oscillator with series feedback. The primary of the transformer is connected in series with the collector and the

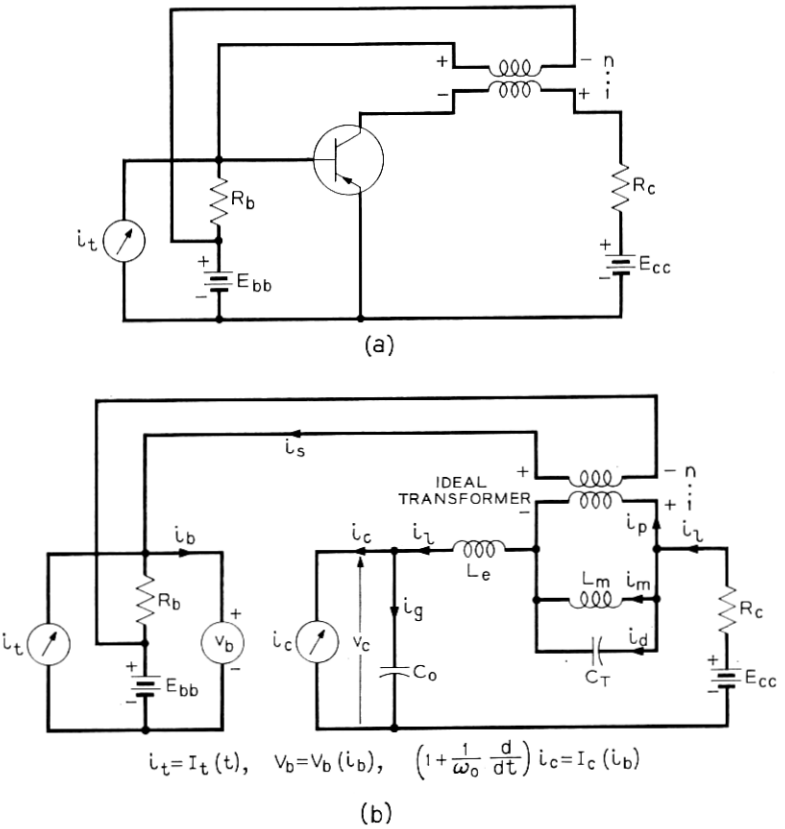

Fig. 3 — (a) Grounded emitter transistor blocking oscillator; (b) nonlinear equivalent circuit.

load resistance, R_c, and its secondary is connected between the base and the bias source E_{bb}. The polarity of the coupling is such that positive feedback exists around the loop when the transistor is conducting. The current generator i_t represents the trigger source and R_b the total external load in the base circuit.* As discussed in the previous section, ω_0 represents the large-signal cutoff frequency of the transistor and is related to ω_α through (8). The capacitance C_0, is the sum of the total stray capacity of the circuit and that of the transistor given by (15). Finally, L_e, L_m and C_T represent, respectively, the leakage and magnetizing inductances and the parasitic capacity of the transformer.

Briefly, the circuit operation is as follows. For monostable operation the bias E_{bb} is selected in such a way that the transistor is cut off at its stable operating point. If a trigger signal of sufficient magnitude and width to bring the circuit into its regenerative region is applied, the collector and base currents will build up until a point in the saturation region is reached. (This point will hereafter be referred to as the "quasi-stable operating point.") Then the magnetizing inductance becomes charged slowly, shorting out more and more of the current fed back to the base. This process will go on until the gain around the loop again becomes equal to unity, at which point the circuit regenerates back into a state of cutoff. Then the energy stored in the transformer slowly dissipates and the circuit recovers to its stable operating point.

The equation governing this complete cycle of operation is derived in Appendix A and normalized in Appendix B.

One point is immediately obvious from these equations: they are extremely long, complicated and relatively useless as they stand. In order to restore the physical feel for the circuit, it will be shown in the remainder of the paper that the equations can be simplified, depending on the region of operation. The primary basis for reducing the more exact equations will be whether or not the base emitter junction is forward- or back-biased. In principle, this approach is similar to that used in piecewise linear analysis. There are several important advantages, however, in starting with the more exact description of the circuit given here. First, retention of the nonlinear terms enables one to determine the operating points of the circuit, which, in turn, give a clear definition of the trigger requirements for reliable operation. Second, the approximations involved in taking the general equations apart can be easily drawn. Finally, the simulation of the blocking oscillator from the exact equations on an analog or digital computer can be readily achieved for purposes of com-

* For convenience, R_b has been placed between base and E_{bb} rather than from base to ground. This approximation serves to eliminate a few small constant terms from the governing equation in Appendix A, and in no way restricts the analysis.

plete analysis or evaluation of the approximations that are made in tearing the more complete description apart. The computer approach also permits the investigation of the effects of the various parameters of the circuit on its response under conditions that can be more closely controlled than can be those in the experimental circuit.

The equations can be broken down in accordance with the importance of the various terms during the following four intervals: (a) "Transition On", (b) "On", (c) "Transition Off" and (d) "Recovery." These will be discussed separately in the following sections.*

IV. THE "TRANSITION ON" INTERVAL

This interval is defined as the time from the initiation of the "On" trigger pulse to the time at which the circuit has apparently come to rest at its quasistable operating point, that is, the time when all transients associated with switching have ceased. Specificially,

$$I_{bc} \lessapprox i_b \lessapprox I_{bs} . \tag{19}$$

By the time triggering occurs, the input impedance to the transistor is low compared to R_b and

$$\frac{V_b(i_b) - E_{bb}}{R_b} \ll i_b , \tag{20}$$

where $[V_b(i_b) - E_{bb}]/n$ represents the voltage drop that must be maintained across the primary of the feedback transformer to overcome the bias and forward drop. This voltage is unavailable in series with the load and should be made as small as possible, implying the use of a transistor with a low forward drop. Fig. 1(b) shows that this voltage is essentially constant during the on interval; therefore very little feedback current will be diverted by the transformer capacity C_T. Subject to condition (20) and the constancy of $[V_b(i_b) - E_{bb}]/n$, this term and derivatives thereof may be neglected. During the switching interval, the contribution from the integral

$$\frac{R_b}{n^2 L_m} \int_0^t \frac{v_b - E_{bb}}{R_b} \, dt$$

will be negligible, since the magnetizing inductance is usually large in

* The equations in Appendix A can be readily modified to deal with the blocking oscillator with shunt feedback. For example, $R_e = 0$ and the load resistance is reflected through the transformer in parallel with R_b.

comparison with the other parameters of the circuit.* Finally, the magnetizing current is equal to nI_{bc}. Therefore, in this interval, (109) of Appendix A simplifies to

$$\frac{L_eC_0}{\omega_0}\frac{d^3i_b}{dt^3}+\left(L_eC_0+\frac{R_eC_0}{\omega_0}\right)\frac{d^2i_b}{dt^2}+\left(\frac{1}{\omega_0}+R_eC_0\right)\frac{di_b}{dt}-(I(i_b)-i_b+I_{bc})$$
$$=\left[1+\left(\frac{1}{\omega_0}+R_eC_0\right)\frac{d}{dt}+\left(L_eC_0+\frac{R_eC_0}{\omega_0}\right)\frac{d^2}{dt^2}+\frac{L_eC_0}{\omega_0}\frac{d^3}{dt^3}\right]I_t(t). \tag{21}$$

The equation governing the equilibrium points (or the "steady-state equation," as it has been called) for this interval is obtained by setting $I_t(t)$ and all the derivatives of i_b equal to zero; that is, we obtain:

$$I(i_b)-i_b+I_{bc}=0, \tag{22}$$

where

$$I(i_b)=\frac{I_c(i_b)}{n}-\left[1+\frac{R_b}{n^2L_m}\left(\frac{1}{\omega_0}+R_eC_0\right)\right]\frac{V_b(i_b)-E_{bb}}{R_b} \tag{23}$$

represents the nonlinear or active part of this equation. In this expression, the term $I_c(i_b)/n$ represents the contribution to $I(i_b)$ by the collector current and the term $[V_b(i_b)-E_{bb}]/R_b$, as noted, is the amount of current flowing down through the resistance R_b to overcome the bias. The term

$$\frac{R_b}{n^2L_m}\left(\frac{1}{\omega_0}+R_eC_0)\right)\frac{V_b(i_b)-E_{bb}}{R_b}$$

represents the modification in $I(i_b)$ due to finite magnetizing inductance, or the equivalent drain of this inductance. In other words, the magnetizing inductance may, as far as the steady-state equation is concerned, be thought of as modifying the resistance R_b to:

$$R_b'=\frac{R_b}{1+\frac{R_b}{n^2L_m}\left(\frac{1}{\omega_0}+R_eC_0\right)}. \tag{24}$$

It is instructive to study the graphical solution of the steady-state equation, since this reveals the locations of the operating points and gives a qualitative idea of the magnitude of the trigger signal needed to trigger the circuit. In Fig. 4 the various components of $I(i_b)$ and the graphical solution of the steady-state equation are shown. For the sake

* The principal effects of neglecting this term are: (a) the trigger current required for reliable triggering will be somewhat larger than indicated in the following for slow trigger signals; (b) the rise time will also increase slightly above that computed in the following, due again to diversion of feedback current through L_m.

of clarity the contribution due to the term containing $V(i_b)$ has been somewhat exaggerated.

In this figure the long-dashed curve represents the dynamic $I_c(i_b)/n$ characteristic for the transistor and the short-dashed curve the contribution due to the $[V(i_b) - E_{bb}]/R_b$ term. The solid curve constitutes the combined effect of these two curves, while the three intersections with the straight line $i_b - I_{bc}$ represent the three operating (or equilibrium) points of the blocking oscillator. Since the loop gain of the circuit

$$T = \frac{dI(i_b)}{di_b} \tag{25}$$

is obviously less than unity at the two extreme points (S and Q.S.), these are operating points of the stable kind. In the following, these two points will be referred to as the "stable" and the "quasistable" operating points, respectively. The circuit cannot stay for an indefinite period of time at the Q.S. point, due to the accumulation of current in the magnetizing

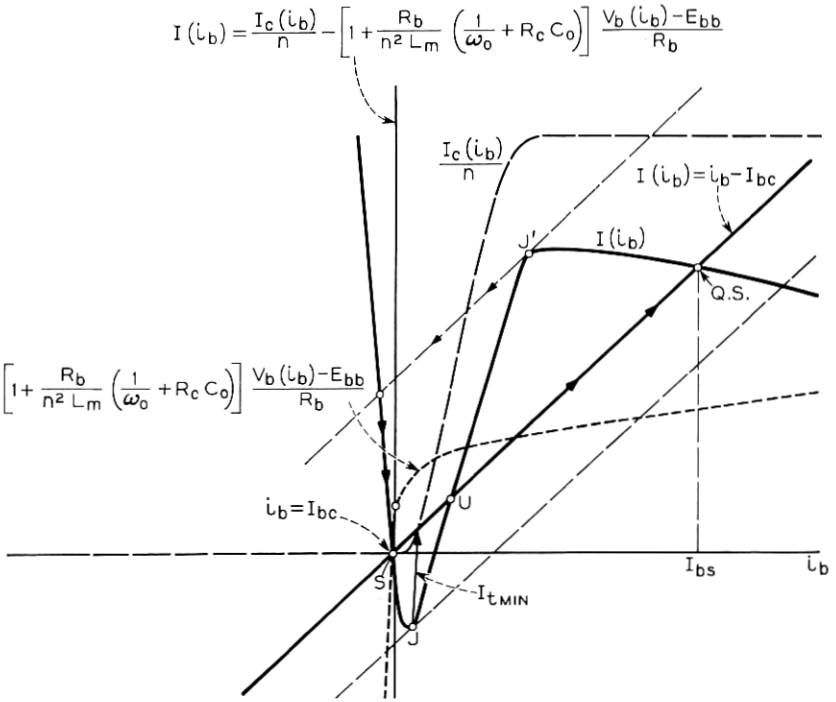

Fig. 4 — Graphical solution of "steady-state equation".

inductance. Finally, the point U is unstable (saddle-point) since the loop gain here is larger than unity, giving rise to responses in the neighborhood of this point directed away from it.

In general, the location of the operating points will depend upon I_{bc}, the shape and magnitude of $I(i_b)$ and the turns ratio n. However, since the contribution to $I(i_b)$ of the term containing $V(i_b)$ is very small when $i_b > 0$ and the backward input resistance $dV(i_b)/di_b$ is very large, the bias current I_{bc} or the bias voltage E_{bb} will not significantly affect the location of any of the operating points, provided the magnetizing inductance is relatively large. In addition, this means that the stable operating point is more or less fixed to a position just to the left of the origin on the i_b axis. Hence, only the locations of the unstable and the quasistable operating points are subject to change; such changes can only be effected by varying $I_c(i_b)$ and n. The magnitudes or saturating values, I_{cs}, of $I_c(i_b)$ and n affect the location of these two points in an opposite manner. For example, as I_{cs} increases or n decreases, the unstable point moves closer to the stable one and the quasistable operating point is displaced further out, provided the value of i_b at which $I_c(i_b)$ saturates remains unchanged. Finally, if $I_c(i_b)$ is made steeper close to the origin, this will also result in a smaller distance between the unstable and the stable operating points.

On the other hand, if the magnetizing inductance, or n, is made very small such that

$$\left[1 + \frac{R_b}{n^2 L_m}\left(\frac{1}{\omega_0} + R_c C_0\right)\right] \frac{V_b(i_b) - E_{bb}}{R_b} \tag{26}$$

is significant with respect to $[I_c(i_b)]/n$, the term containing $V_b(i_b)$ will also affect the location of the unstable and the quasistable operating points. For instance, by reducing L_m (but letting n remain fixed) the $I(i_b)$ curve is moved downward, causing the unstable operating point to move further away and the quasistable one to move closer to the stable operating point, thereby reducing the range that i_b and $I(i_b)$ traverse in going from one operating point to the other.

The dependence upon n is more complicated, however, since it affects both the saturation value of $I(i_b)$ and $n^2 L_m$. If n is very small, $n^2 L_m$ will also be small, tending to make the distance between the stable and unstable points large. On the other hand, a small n will also increase the saturation value of $I(i_b)$, thereby tending to decrease the distance between these two points. However, since $n^2 L_m$ is proportional to the square of n, while I_s varies as $1/n$, the net effect at first will be that the unstable operating point will move closer to the stable one when n is increased

from a small initial value. Then, as n becomes larger, the effect of the $V(i_b)$ term becomes negligible and $I_c(i_b)/n$ will predominate, with the result that the distance between these two operating points will increase. Hence, as a function of n, this distance will go through a minimum. Therefore, in order to make sure that the magnetizing inductance does not affect the location of the operating points and does not become significantly charged during the "Transition On" interval, L_m and n should be selected well beyond this minimum; that is,

$$n^2 - \frac{I_c(i_b)}{\dfrac{V_b(i_b) - E_{bb}}{R_b}} n + \frac{R_b}{L_m}\left(\frac{1}{\omega_0} + R_c C_0\right) \ll 0 \tag{27}$$

In such cases, it is an excellent approximation to neglect the effect of the term containing $V_b(i_b)$ entirely, and use only $I_c(i_b)/n$ for $I(i_b)$. The graphical determination of the operating points then simplifies to that of Fig. 5. It is seen that n is now simply equal to the ratio, $I_{cs}/(I_{bs} - I_{bc})$, which, by virtue of (8), means that ω_0 may be expressed in terms of ω_α and n only; that is,

$$\omega_0 = \frac{\omega_\alpha}{1 + n}. \tag{28}$$

In the following, the requirements for triggering the blocking oscillator, the effect of trigger magnitude, the shape of the collector current charac-

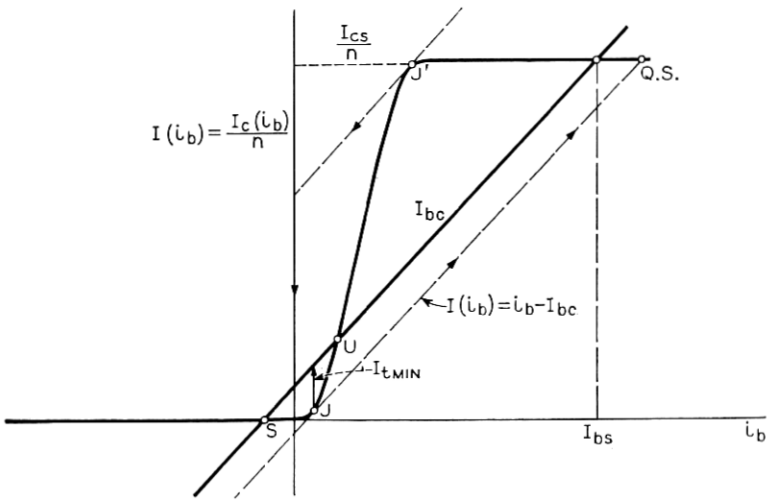

Fig. 5 — Approximate location of operating points.

teristics and the coefficients of the differential equation upon rise time and delay and the conditions for a nonoscillatory response will all be discussed. It will be assumed that condition (27) is satisfied, so that the effect of the magnetizing inductance may be neglected. Also, for most of the following, $I_c(i_b)$ will be approximated by an analytic function.

These items are most easily discussed if (21) is written in normalized form. From Appendix B, it can be shown that the normalized equation governing the "Transition On" interval is

$$a^2 \frac{d^3x}{d\tau^3} + (a^2 + b) \frac{d^2x}{d\tau^2} + (1 + b) \frac{dx}{d\tau} + x - f(x) = \left[1 + (1 + b) \frac{d}{d\tau} + (a^2 + b) \frac{d^2}{d\tau^2} + a^2 \frac{d^3}{d\tau^3}\right] g(\tau), \tag{29}$$

where all symbols are defined in Appendix B. The normalized steady-state equation is now

$$f(x) - x = 0, \tag{30}$$

where both x and $f(x)$ attain the values 0 and 1 at the stable and the quasistable operating points, respectively. Finally, the normalized output voltage for this interval may be written

$$y = x - g(\tau). \tag{31}$$

V. TRIGGER SIGNAL REQUIREMENTS

If the blocking oscillator is released from an initial position that is different from any of its operating points, it will proceed, depending upon the initial conditions, either to the stable or the quasistable operating point. For instance, if the initial values of all the derivatives in (29) are equal to zero, the circuit will simply come to rest at the operating point that is on the same side of the unstable point as is the initial position. In general, however, the circuit may cross the unstable operating point, provided the initial values of some of the derivatives in (29) are large enough. Hence, in order to make the blocking oscillator flip over from the stable to the quasistable operating point, the applied trigger signal must have sufficient magnitude and duration either to bring the circuit past its unstable operating point or to impart energy into it so that the initial values of the derivatives in (29) are large enough to make the circuit traverse the unstable point by itself. In this section the conditions this requirement imposes upon the trigger signal will be discussed.

The simplest possible case is that of a trigger signal with a very large width. In such cases, the trigger pulse will vary very slowly or be nearly

constant during the transition interval, and the derivatives of $g(\tau)$ in (29) may therefore be neglected. Up to the point of triggering, the base current will also vary very slowly and its derivatives will consequently be small.* Therefore, prior to the time regenerative action takes place, (29) reduces to:

$$x - f(x) = g(\tau). \tag{32}$$

Under these conditions, the trigger signal acts mainly as a variable bias causing the load line in Fig. 4 or Fig. 5 to be displaced to the right. This, in turn, makes the stable and the unstable operating points move closer and closer together until they merge into one point. At this point (J) the load line is tangential to $f(x)$ [or $I(i_b)$] and an infinitesimal additional displacement of the load line will cause the circuit to have only one possible operating point. Hence, a "jump" to the quasistable operating point will take place at this point, and the minimum required trigger magnitude is given by:

$$G_{\min} = x_j - f(x_j), \tag{33}$$

where x_j represents the value the normalized base current has at the point of tangency, J; that is, x_j is found by solving the equation:

$$\frac{df(x_j)}{dx_j} = 1. \tag{34}$$

In terms of actual trigger current, this minimum corresponds to the vertical distance, $I_{t\,\min}$, between the point of tangency and the load line, as shown in Figs. 4 or 5. The variation of $I_{t\,\min}$ with n will proceed in the same manner as for the distance between the stable and unstable operating points. This effect will be described more fully in the following.

When more rapidly varying trigger signals are applied to the blocking oscillator, the terms containing derivatives of $g(\tau)$ and x become so large that they must be taken into account. Since (29) is both nonlinear and inhomogeneous, no analytical solution exists, and it is therefore impossible to derive in closed form conditions that the trigger signal must satisfy for reliable operation. Hence, numerical methods or analog computer solutions must be resorted to. In the particular case, where the magnitude required to trigger the circuit for a particular fixed width of the trigger pulse must be found, the latter method was chosen, because repeated adjustments of parameters until the desired solution is obtained are much more readily accomplished on an analog computer.

* The quantitative definition of "small" is, of course, dependent on the coefficients (circuit parameters) multiplying the various derivatives.

To prevent overload of amplifiers and integrators and also to simplify the analog computer setup, (29) was first rewritten in terms of the normalized output voltage, y, which simplifies it to:

$$a^2 \frac{d^3y}{d\tau^3} + (a^2 + b) \frac{d^2y}{d\tau^2} + (1 + b) \frac{dy}{d\tau} + y = f[y + g(\tau)]. \quad (35)$$

The Gaussian pulse was used as a representative trigger signal; that is,

$$g(\tau) = Ge^{-[(\tau-\tau_0)/0.6\tau_w]^2}, \quad (36)$$

where G is the magnitude, τ_w the 50 per cent width and τ_0 the time at which $g(\tau)$ attains its maximum value, G. For $f(x) = f[y + g(\tau)]$, representing the normalized relationship between collector current and base current, the analytical function

$$f(x) = \frac{x^2}{2x^2 - 2x + 1} \quad (37)$$

was chosen. This choice was dictated strictly on the basis of mathematical simplicity and tractability of the solution of (35) when g, a and b are zero. This function is depicted by the solid line in Fig. 6, from which it can be seen that it has a minimum at $x = 0$ and a maximum $x = 1$, where it is equal to zero and unity, respectively. Also, $f(x)$ has an inflection point at $x = \frac{1}{2}$ around which it is symmetrical. The slope of $f(x)$ at this point is equal to 2. For values of x less than zero and larger than one it is slowly asymptotic to the horizontal line $\frac{1}{2}$. The normalized

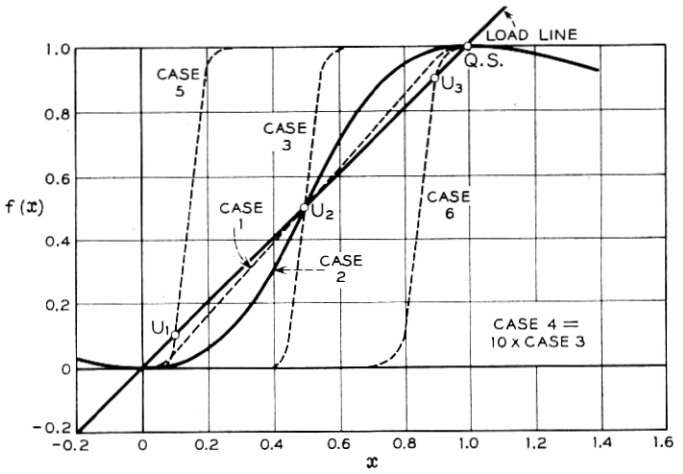

Fig. 6 — Various nonlinear characteristics.

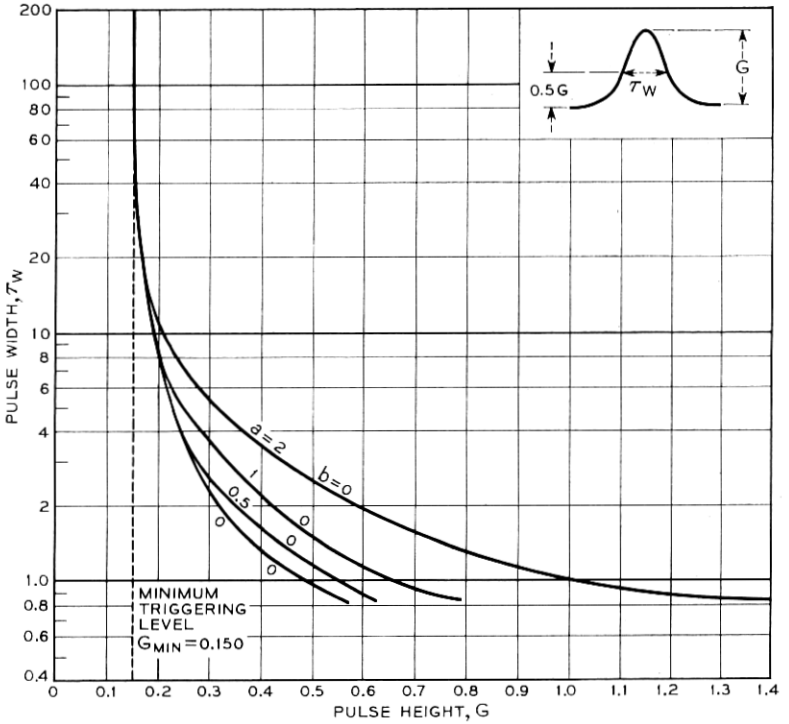

Fig. 7 — Relationships between magnitude and width of applied signal required to trigger the blocking oscillator with $b = 0$.

load line of the circuit is also shown in Fig. 6. It intersects $f(x)$ at the points x equal to 0, $\frac{1}{2}$ and 1, and these are therefore the stable, unstable and quasistable operating points, respectively. Although the function $f(x)$ differs from a real i_c/i_b characteristic in that it is not constant beyond the stable and the quasistable operating points, it resembles such a characteristic sufficiently closely within the region of interest. Hence, solutions of (35) having reasonable overshoots should be expected to approximate exact ones very closely and exhibit the main features of the circuit accurately.

On the analog computer the following procedure was used. The circuit was assumed to be at rest at the stable operating point prior to the application of the trigger pulse, and the initial value of all the derivatives was set equal to zero. Then, for each value of the width τ_w, the magnitude G was adjusted so that the response barely flipped over to the quasistable operating point. The resulting relationship between the

magnitude and width of the trigger pulse is shown in Figs. 7 and 8 for various values of the parameters a and b. It is seen that the curves are somewhat hyperbolic in shape and that all of them are asymptotic to the vertical line $G_{\min} = 0.15$ at large pulse widths. This asymptote corresponds exactly to the minimum trigger magnitude given by (33) and, indeed, if the expression for $f(x)$ from (37) is substituted into (33) and (34), the result is $G_{\min} = 0.1504$, which agrees quite closely with the computed value. From Figs. 7 and 8 it can be seen that, at large pulse widths, the critical trigger magnitude is nearly independent of a and b. As the width becomes smaller, a larger magnitude is required to trigger

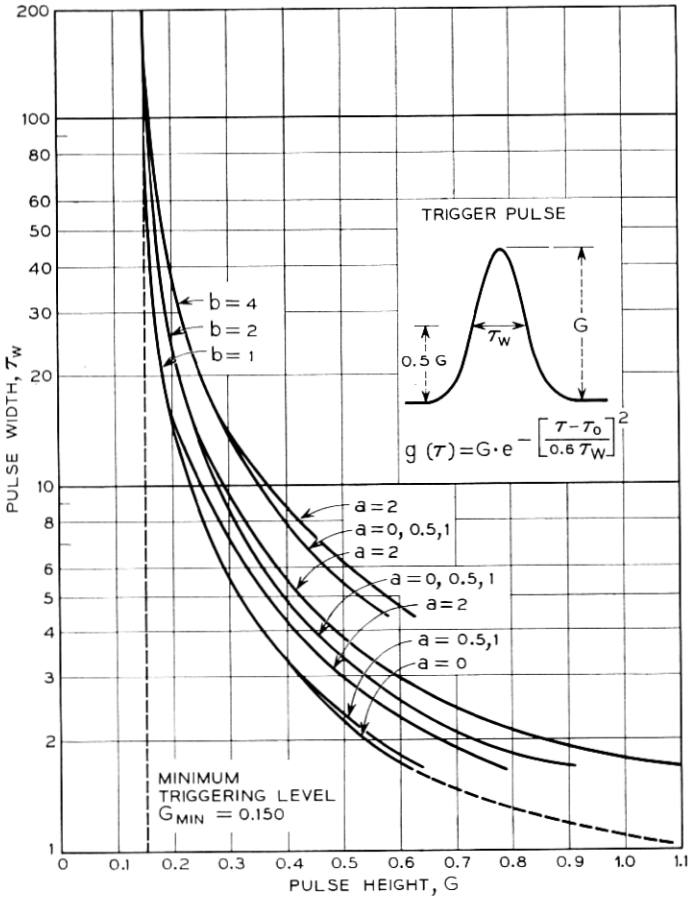

Fig. 8 — Relationships between magnitude and width of applied signal required to trigger the blocking oscillator with $b = 1$, 2 and 4.

TABLE II

τ_w	$b = 0$				$b = 1$				$b = 2$				$b = 4$			
	$a = 0$	$a = 0.5$	$a = 1.0$	$a = 2.0$	$a = 0$	$a = 0.5$	$a = 1.0$	$a = 2.0$	$a = 0$	$a = 0.5$	$a = 1.0$	$a = 2.0$	$a = 0$	$a = 0.5$	$a = 1.0$	$a = 2.0$
0.835	$G =$ 0.57	$G =$ 0.625	$G =$ 0.79	$G =$ 1.4	$G =$ 1.7	$G =$ 1.7	$G =$ 1.7									
	$N =$ 0.3507	$N =$ 0.3966	$N =$ 0.5344	$N =$ 1.0438	$N =$ 1.2943	$N =$ 1.2943	$N =$ 1.2943									
1.67	$G =$ 0.35	$G =$ 0.40	$G =$ 0.47	$G =$ 0.67	$G =$ 0.61	$G =$ 0.64	$G =$ 0.64	$G =$ 0.79	$G =$ 0.91	$G =$ 0.91	$G =$ 0.91	$G =$ 1.1				
	$N =$ 0.334	$N =$ 0.4175	$N =$ 0.5344	$N =$ 0.8684	$N =$ 0.7682	$N =$ 0.8183	$N =$ 0.8183	$N =$ 1.0688	$N =$ 1.2692	$N =$ 1.2692	$N =$ 1.2692	$N =$ 1.5865				
4.175	$G =$ 0.24	$G =$ 0.24	$G =$ 0.28	$G =$ 0.335	$G =$ 0.34	$G =$ 0.34	$G =$ 0.34	$G =$ 0.39	$G =$ 0.423	$G =$ 0.423	$G =$ 0.423	$G =$ 0.45	$G =$ 0.58	$G =$ 0.58	$G =$ 0.58	$G =$ 0.605
	$N =$ 0.3758	$N =$ 0.3758	$N =$ 0.5428	$N =$ 0.7724	$N =$ 0.7933	$N =$ 0.7933	$N =$ 0.7933	$N =$ 1.0020	$N =$ 1.1398	$N =$ 1.1398	$N =$ 1.1398	$N =$ 1.2525	$N =$ 1.7953	$N =$ 1.7953	$N =$ 1.7953	$N =$ 1.8996
6.68	$G =$ 0.215	$G =$ 0.215	$G =$ 0.215	$G =$ 0.27	$G =$ 0.28	$G =$ 0.28	$G =$ 0.28	$G =$ 0.32	$G =$ 0.328	$G =$ 0.328	$G =$ 0.328	$G =$ 0.36	$G =$ 0.433	$G =$ 0.433	$G =$ 0.433	$G =$ 0.47
	$N =$ 0.4342	$N =$ 0.4342	$N =$ 0.4342	$N =$ 0.8016	$N =$ 0.8684	$N =$ 0.8684	$N =$ 0.8684	$N =$ 1.1356	$N =$ 1.1890	$N =$ 1.1890	$N =$ 1.1890	$N =$ 1.4028	$N =$ 1.8904	$N =$ 1.8904	$N =$ 1.8904	$N =$ 2.1376
8.35	$G =$ 0.2	$G =$ 0.2	$G =$ 0.2	$G =$ 0.235	$G =$ 0.225	$G =$ 0.225	$G =$ 0.225	$G =$ 0.285	$G =$ 0.31	$G =$ 0.31	$G =$ 0.31	$G =$ 0.325	$G =$ 0.4	$G =$ 0.4	$G =$ 0.4	$G =$ 0.43
	$N =$ 0.4175	$N =$ 0.4175	$N =$ 0.4175	$N =$ 0.7098	$N =$ 0.6263	$N =$ 0.6263	$N =$ 0.6263	$N =$ 1.1273	$N =$ 1.3360	$N =$ 1.3360	$N =$ 1.3360	$N =$ 1.4613	$N =$ 2.0875	$N =$ 2.0875	$N =$ 2.0875	$N =$ 2.3380
16.70	$G =$ 0.17	$G =$ 0.17	$G =$ 0.17	$G =$ 0.17	$G =$ 0.19	$G =$ 0.19	$G =$ 0.19	$G =$ 0.19	$G =$ 0.224	$G =$ 0.224	$G =$ 0.224	$G =$ 0.224	$G =$ 0.27	$G =$ 0.27	$G =$ 0.27	$G =$ 0.27
	$N =$ 0.3340	$N =$ 0.3340	$N =$ 0.3340	$N =$ 0.3340	$N =$ 0.6680	$N =$ 0.6680	$N =$ 0.6680	$N =$ 0.6680	$N =$ 1.2358	$N =$ 1.2358	$N =$ 1.2358	$N =$ 1.2358	$N =$ 2.0040	$N =$ 2.0040	$N =$ 2.0040	$N =$ 2.0040
41.75	$G =$ 0.159	$G =$ 0.159	$G =$ 0.159	$G =$ 0.159	$G =$ 0.167	$G =$ 0.167	$G =$ 0.167	$G =$ 0.167	$G =$ 0.175	$G =$ 0.175	$G =$ 0.175	$G =$ 0.175	$G =$ 0.195	$G =$ 0.195	$G =$ 0.195	$G =$ 0.195
	$N =$ 0.3758	$N =$ 0.3758	$N =$ 0.3758	$N =$ 0.3758	$N =$ 0.7098	$N =$ 0.7098	$N =$ 0.7098	$N =$ 0.7098	$N =$ 1.0438	$N =$ 1.0438	$N =$ 1.0438	$N =$ 1.0438	$N =$ 1.8788	$N =$ 1.8788	$N =$ 1.8788	$N =$ 1.8788
83.50	$G =$ 0.151	$G =$ 0.151	$G =$ 0.151	$G =$ 0.151	$G =$ 0.152	$G =$ 0.152	$G =$ 0.152	$G =$ 0.152	$G =$ 0.157	$G =$ 0.157	$G =$ 0.157	$G =$ 0.157	$G =$ 0.165	$G =$ 0.165	$G =$ 0.165	$G =$ 0.165
	$N =$ 0.0835	$N =$ 0.0835	$N =$ 0.0835	$N =$ 0.0835	$N =$ 0.1670	$N =$ 0.1670	$N =$ 0.1670	$N =$ 0.1670	$N =$ 0.5845	$N =$ 0.5845	$N =$ 0.5845	$N =$ 0.5845	$N =$ 1.2525	$N =$ 1.2525	$N =$ 1.2525	$N =$ 1.2525
167.0	$G =$ 0.151	$G =$ 0.151	$G =$ 0.151	$G =$ 0.151	$G =$ 0.151	$G =$ 0.151	$G =$ 0.151	$G =$ 0.151	$G =$ 0.151	$G =$ 0.151	$G =$ 0.151	$G =$ 0.151	$G =$ 0.151	$G =$ 0.151	$G =$ 0.151	$G =$ 0.151
	$N =$ 0.1670	$N =$ 0.1670	$N =$ 0.1670	$N =$ 0.1670	$N =$ 0.1670	$N =$ 0.1670	$N =$ 0.1670	$N =$ 0.1670	$N =$ 0.1670	$N =$ 0.1670	$N =$ 0.1670	$N =$ 0.1670	$N =$ 0.1670	$N =$ 0.1670	$N =$ 0.1670	$N =$ 0.1670
$\overline{N}$	0.3746	0.3931	0.4533	0.7008	0.8183	0.8255	0.8255	0.9518	1.2023	1.2023	1.2023	1.3305	1.9312	1.9312	1.9312	2.0516

the circuit and this magnitude increases with a and b. The curves indicate a stronger dependence of G upon b than upon a, meaning that the output capacitance and the load resistance affect the trigger sensitivity of the circuit more than the leakage inductance does.

The fact that the curves in Figs. 7 and 8 resemble hyperbolas suggests that the product of the pulse width and the difference between the magnitude and its minimum value is nearly constant; that is,

$$(G - G_{\min})\tau_w \doteq N(a, b), \tag{38}$$

where N is a function of a, b and the nonlinear characteristic. To investigate this further, the above product was formed for all the measurements taken, and the results are shown in Table II. It is seen that the value that N assumes for each measurement varies randomly around its mean value with no consistent deviation in any direction, except at large pulse widths, where it is quite small, and at short pulse widths, where it is quite large. Taking into account the subjectiveness involved in determining the point at which the response barely flips over to the quasi-stable operating point, the accuracy of the computer and the fact that at large pulse widths the value of G is very nearly equal to $G_{\min}$, it must be concluded that (38) is indeed a good approximation over particular regions of τ_w. Since the area of the Gaussian pulse in (36) is

$$A = \int_{-\infty}^{\infty} g(\tau)d\tau = \sqrt{\pi}G\tau_w, \tag{39}$$

it can be concluded that the area of an equivalent trigger pulse of magnitude $(G - G_{\min})$, not the area of the actual trigger pulse, stays approximately constant for given values of a and b. This brings out the fact that the blocking oscillator is not strictly an amplitude threshold device, but an energy threshold device.

The data given in Table II can be closely approximated by a function of the form

$$N(a, b) = K_0 + K_1 a + K_2 b. \tag{40}$$

For $1.67 \leqq \tau_w \leqq 41.75$, and $b \neq 0$, these values are: $K_0 = 0.38$, $K_1 = 0.06$, $K_2 = 0.42$. With these values in (40), the computed $N(a, b)$ agrees with the tabulation in Table II to within better than 30 per cent. In addition to the inaccuracies introduced by the computer and operator when G is close to $G_{\min}$, it is to be expected that, at the largest pulse widths, $N(a, b)$ will be independent of both a and b. For $\tau_w = 167$, Table II confirms the contention that the very slow trigger signal acts strictly to vary the bias. When τ_w is between 16.70 and 83.5, $N(a, b)$ is independent

of a for the range of parameters covered. Only the coefficients of the second and third derivatives with respect to the base current are functions of a. Therefore it can be concluded that this range of τ_w covers a transition region where only the first derivative term (ω_0 and collector capacity) is important. At the other extreme — the very narrow trigger pulse — the dependence on a is larger than indicated by the value of K_1 derived for the region $1.67 \leqq \tau_w \leqq 41.75$. Here the dependence on the higher derivatives (leakage inductance) is more pronounced, again confirming our physical reasoning.

The case $b = 0$ is of little practical concern, since this corresponds to an undamped output circuit working into a short-circuited load.

Other implications of the relationship between trigger magnitude and width can be brought out more clearly if we examine the unnormalized version of (40). If we substitute (40) in (38), neglect the weak dependence on leakage inductance, neglect parasitic capacity from collector to ground, and substitute from the normalizing equations, we get

$$(I_t - I_{t\,\min})T_w = \left(\frac{I_{cs}}{n} - I_{bc}\right)(1 + n)\left(\frac{K_0}{\omega_\alpha} + K_2\, 1.5C_cR_c\right). \tag{41}$$

From this relationship it can be seen that the magnitude-width product decreases as ω_α is increased until K_0/ω_α can be neglected with respect to $K_2\, 1.5C_cR_c$. This dependence on ω_α can also be viewed in an equivalent manner. Since K_0 and K_2 are both about equal to 0.4, (41) can be written in the following form

$$(I_t - I_{t\,\min})T_w \doteq \left(\frac{I_{cs}}{n} - I_{bc}\right) K_0 \frac{(1 + b)}{\omega_0}. \tag{42}$$

It will be recalled, from the discussions on the equivalent circuit for the transistor, specifically (18), that $(1 + b)/\omega_0$ is a good approximation to the large-signal (saturating step) delay time of the resistively loaded common emitter stage. Therefore (42) can be written

$$(I_t - I_{t\,\min})T_w \doteq K_0\left(\frac{I_{cs}}{n} - I_{bc}\right) T_0. \tag{43}$$

As ω_α is increased, the delay time of the basic transistor stage (T_0) without external feedback decreases. In the blocking oscillator this is equivalent to a reduction of one of the time constants in the positive feedback loop, thereby permitting a more rapid build-up of the regenerative loop, or, alternately, regeneration can occur for a lower trigger signal for a given trigger width.

The dependence of this product on n is more difficult to visualize, since K_0, K_1 and K_2 are functions of the circuit operating points, which in turn are dependent on n. As mentioned previously, $I_{t\,\min}$ will vary with n in much the same way that the distance between the stable and unstable operating point varies with n. For small n, $I_{t\,\min}$ will be large and decrease to a minimum as n increases, and then begin to increase with n. This can be seen from the graphical construction of Figs. 4 and 5, and it has also been observed experimentally. It is reasonable to expect that the product given by (42) will vary in a similar manner, though no rigorous proof can be given here.

For trigger signals that are nonzero over only a finite time interval, a relationship between magnitude and width similar to that shown in Figs. 7 and 8 exists. The principal difference is that the curves corresponding to those of Fig. 7 or 8 are now asymptotic to a finite value of width as well as of magnitude. In other words, for such trigger signals there exists a minimum width, $\tau_{w\,\min}$, below which the blocking oscillator cannot be triggered even when the magnitude of the trigger pulse is made infinite. That such a minimum width exists can be easily realized by considering (35) when a square pulse of infinite magnitude is applied to the circuit. In such a case, the collector current generator will saturate immediately, making $f[y + g(\tau)] = 1$. Hence, the actual forcing function is finite even if the magnitude of $g(\tau)$ is infinite, and the applied trigger pulse must therefore have a finite width in order to make the circuit flip over to its quasistable operating point. The reason $\tau_{w\,\min}$ is not finite in the case of the Gaussian pulse is the fact that this function is nonzero except at infinity. Thus, the width of $g(\tau)$ must be zero in order to make the duration of the actual forcing function finite.

These considerations may be used to calculate $\tau_{w\,\min}$. As an example, let us consider the case when $a = b = 0$. The solution to (35) for $\tau \leqq \tau_{w\,\min}$ is then simply

$$y(\tau) = 1 - e^{-\tau}, \tag{43}$$

and the minimum width is now the time sufficient to bring y up to the unstable operating point; that is, $y = \frac{1}{2}$. This gives $\tau_{w\,\min} = 0.693$. In the more general case, when a and b are nonzero, the procedure is somewhat more complicated. It involves finding first the relationship between y and its first and second derivatives necessary to slide the circuit past its unstable operating point when $g(\tau)$ is zero, and then determining the width that will make these quantities satisfy this relationship. Since this procedure is usually quite laborious, it is more practical to estimate $\tau_{w\,\min}$ from two points on the magnitude-width curves.

VI. DELAY AND RISE TIME

The delay and rise time of the blocking oscillator are, in general, dependent upon all parameters in the circuit. The most important of these are the magnitude and width of the trigger signal, the shape of the i_c/i_b characteristic, the cutoff frequency ω_0 (or ω_α and n) and, finally, the collector capacitance in conjunction with the load resistance and the leakage inductance. To see clearly how each particular parameter affects the delay and rise time, these will be discussed separately, although it may not be possible to vary some of them independently in the actual physical circuit. In the following, the delay time is defined as the time difference between the maximum of the trigger pulse and the 50 per cent point of the normalized output. The rise time is the time required for the output to traverse 10 to 90 per cent of its final value.

6.1 *The Effect of Trigger Magnitude and Width*

It is instructive to consider first the transient responses when the blocking oscillator is simply released from various initial positions. In such cases these responses are obtained from (35) by setting $g(\tau) = 0$ and assigning initial values to y and its derivatives. In particular, if the collector capacitance and the leakage inductance are so small that they may be neglected, an analytical expression for these responses may be obtained. If we limit ourselves to this particular case by setting $a = b = 0$ in (35) and using the analytical approximation to the i_c/i_b characteristic, the solution to this equation becomes (by simple separation of variables)

$$\frac{y(y-1)}{y-0.5} = \frac{y(0+)[y(0+)-1]}{y(0+)-0.5}\, e^{-\tau}, \tag{44}$$

where $y(0+)$ represents the initial value of y. The bistable nature of the blocking oscillator is reflected in (44), because, as $\tau \to \infty$, y approaches either the stable ($y = 0$) or the quasistable ($y = 1$) operating point. Which one it will attain in an actual case depends upon whether the initial position is below or above the unstable operating point. In the neighborhood of the point ($y = 0.5$) the output voltage becomes an exponential ascending function of time, thereby exhibiting the unstable characteristic of this point. Fig. 9 shows the responses of (44) for six initial values located between the unstable and the quasistable operating points.[12] It is seen that, as the initial value of y is decreased toward the unstable operating point, the delay and rise time of the circuit become larger, increasing rapidly as $y(0+)$ approaches this point. To minimize

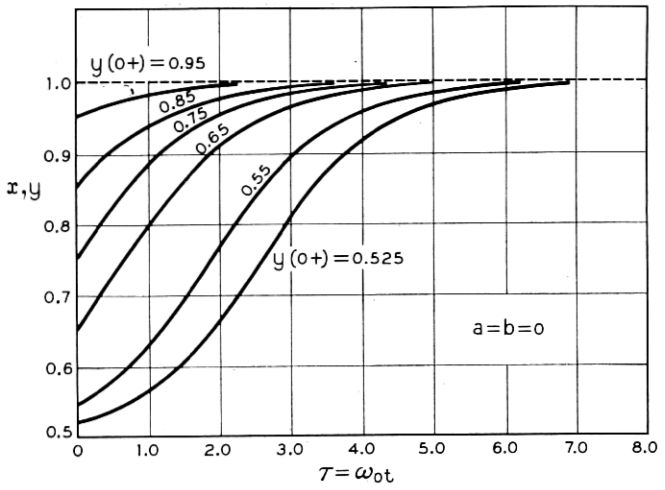

Fig. 9 — Normalized time response of the blocking oscillator when the circuit is released from various initial positions.

rise time, the magnitude and width of the trigger signal should at least be such that the circuit has been brought well beyond the unstable point when the trigger terminates.

When the coefficients a and b (or the trigger function) are not equal to zero, (44) cannot be solved analytically and numerical methods must be used. In Fig. 10 the results of solving this equation by the Runge-Kutta method on a digital computer are shown. Again, the analytical approximation to the i_c/i_b characteristics was used and the Gaussian function represented the trigger signal. To conform with values encountered in a particular circuit, a and b were, in all of these cases, made equal to 0.447 and 0.8, respectively. In the first of these figures, Fig. 10(a), the normalized response of the base current, x, and the output voltage, y, to a slow trigger pulse, are shown. It is seen that the output voltage does not change appreciably until $g(\tau)$ reaches the critical triggering level, which, from Table II, is equal to 0.167 for $\tau_w = 41.75$. Subsequently, the output voltage switches rapidly in comparison to the trigger signal to the quasistable operating point. Hence, one should expect, in the case of a slow trigger signal, that the rise time of the blocking oscillator is more or less independent of the trigger magnitude as long as this magnitude is larger than the critical value necessary to activate the circuit. The upper curve in Fig. 11 bears out this statement. Here, the rise time is shown as a function of pulse magnitude, and it is seen that, except for a trigger magnitude close to the critical triggering level, the rise time is

virtually constant over the whole range. Thus, one may conclude that in this case the rise time is, practically speaking, dependent only upon the parameters of the blocking oscillator itself. The delay time, on the other hand, will of course vary with trigger magnitude, but only to the extent of the time it takes the trigger signal to reach the critical triggering level.

Figs. 10(b) through 10(d) show the response of the blocking oscillator to a short trigger pulse of successively increasing magnitude. Actually, in all figures except Fig. 10(c) two trigger pulses were applied, one that

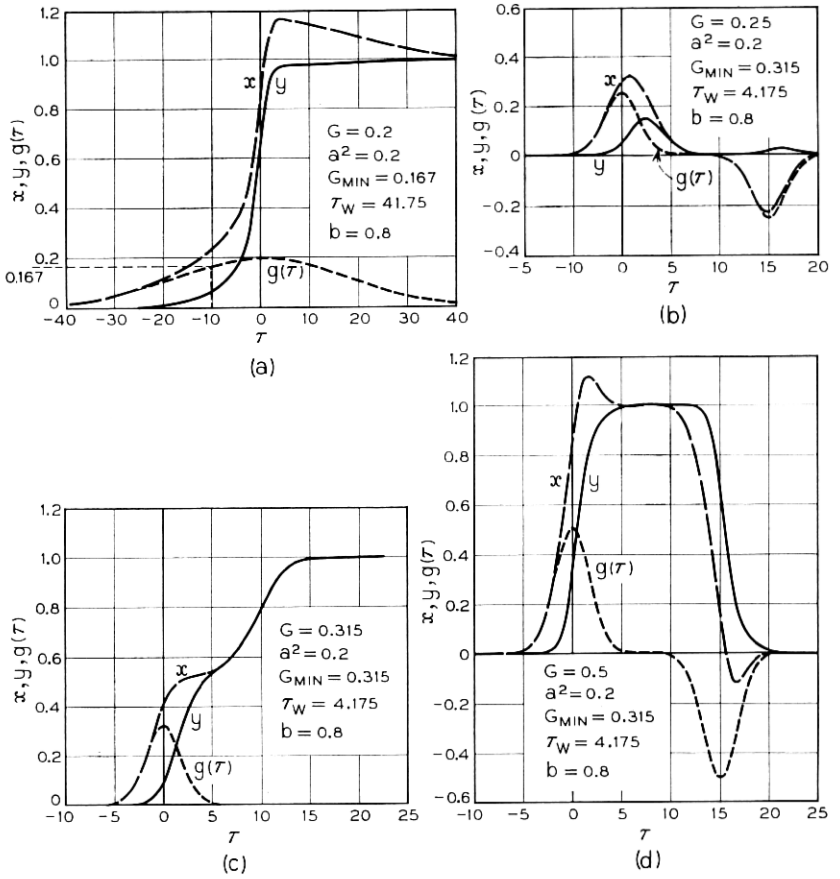

Fig. 10 — Computed responses of the blocking oscillator to trigger pulses of various widths and magnitudes: (a) slow trigger pulse; (b) inadequate trigger pulse; (c) trigger pulse having just limiting magnitude; (d) adequate trigger pulse.

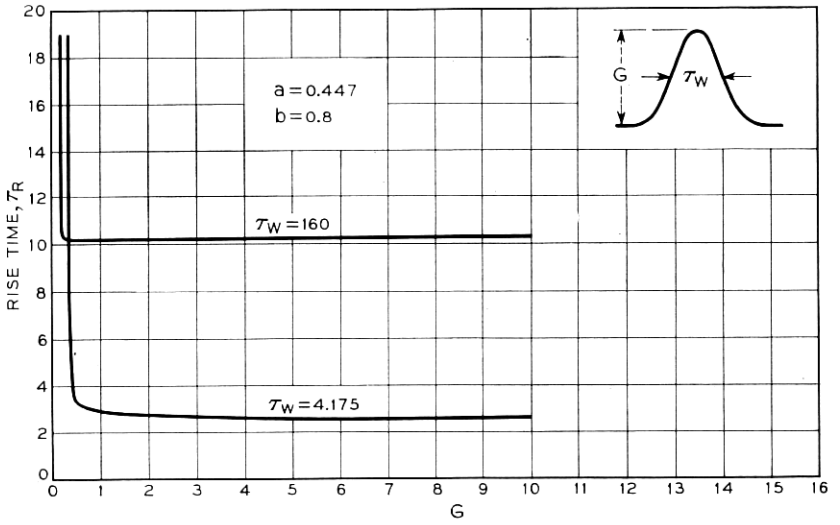

Fig. 11 — Rise time as a function of trigger pulse magnitude.

turns the blocking oscillator "on", followed by another that turns it "off". This was done in order to simulate the conditions for a blocking oscillator that might be used in a regenerative repeater. In Fig. 10(b) the magnitude of the trigger signal was insufficient to activate the blocking oscillator, while in Fig. 10(c) it was just barely large enough to make the circuit flip over to the quasistable operating point. The rather large rise time and the inflection point at $y = 0.5$ should be noted in the latter case, which, as explained previously, is due to the fact that the circuit is now essentially released from a position close to the unstable operating point. As the magnitude is increased further the rise time at first decreases rapidly and then levels off, approaching a limit for large values of G. This is depicted by the lower curve in Fig. 11. In this case the rise time is largely independent of trigger magnitude as long as the magnitude is at least 50 per cent larger than the critical triggering level. It should be pointed out, however, that the apparent leveling off of the rise time in the fast pulse case is only true when ω_0 may be considered to be independent of trigger magnitude. If a fast and large trigger pulse is applied such that the base current significantly exceeds the value I_{bs} during transition, the maximum value of this current should, according to (7), be used to calculate ω_0 rather than I_{bs}. This results in a larger ω_0 and therefore a smaller rise time than that indicated by Fig. 11. The correction to be applied to ω_0 in such cases is, by virtue of (6) and (8), equal to:

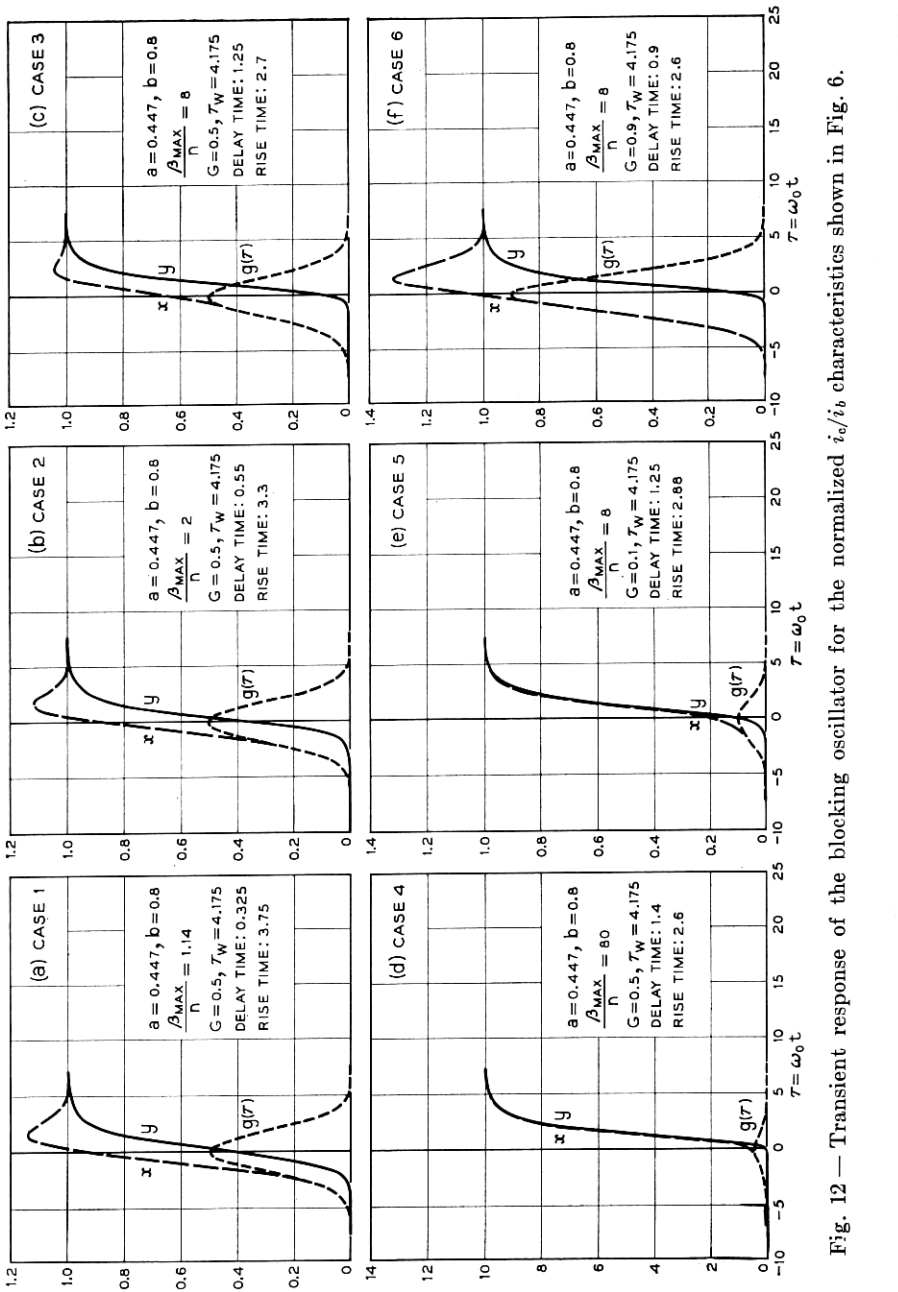

Fig. 12 — Transient response of the blocking oscillator for the normalized i_c/i_b characteristics shown in Fig. 6.

$$\frac{\omega_0'}{\omega_0} = \frac{1 + \dfrac{I_{cs}}{I_{bs} - I_{bc}}}{1 + \dfrac{I_{cs}}{I_{b\max} - I_{bc}}} = \frac{1 + n}{1 + \dfrac{n}{x_{\max}}}. \tag{45}$$

In most practical blocking oscillators, however, the stable and unstable operating points are located very close together, so that such correction is rarely needed. Also, the desirability of a large power gain favors the use of a design requiring only small trigger magnitudes. Finally, in the case of a slow trigger signal, such correction is never needed, since here the trigger signal does not change appreciably during the relatively fast transition from the stable to the quasistable operating point.

6.2 *The Effect of the Shape of the i_c/i_b Characteristic*

To see how the shape of the i_c/i_b characteristic affected the delay and the rise time of the blocking oscillator, transient responses were computed from (35) using for $f(x)$ the functions depicted in Fig. 6. In all cases, the location of the stable operating point was kept fixed and the circuit was assumed to be initially at rest at this point. To trigger the circuit a Gaussian pulse was used which had a 50 per cent width of 4.175 and a magnitude in each case equal to the distance between the stable and unstable operating points. In all cases, $a = 0.447$ and $b = 0.8$.

In the first set of computations the location of the unstable operating point was kept fixed while the slope of the characteristic through this point was varied by using four different functions for $f(x)$. These are the cases numbered 1 through 4 in Fig. 6, the fourth one being essentially Case 3 multiplied by ten. The slope at the unstable operating point at each of these cases, which on an unnormalized scale represents $\beta_{\max}/n$ of the circuit, are, respectively, 1.14, 2, 8 and 80. However, the average value of β/n is the same in all cases, since the quasistable operating point is located at (1, 1) in the first three cases and at (10, 10) in the last one. Figs. 12(a) through 12(d) give the results of computing the transient response from (44) in each of these cases. In Fig. 13 the rise time is plotted as a function of $\beta_{\max}/n$. It is seen that the delay and rise time change only slightly over the whole range of $\beta_{\max}/n$; the most rapid variation being confined to the region where $\beta_{\max}/n$ is nearly equal to unity. The slope must be greater than this value for $f(x)$ to intersect the load line at three points. Hence, it can be concluded that the rise time decreases very little when $\beta_{\max}/n$ is increased, as long as this quantity is larger than unity. In fact, Fig. 13 shows that a 70-to-1 change in loop gain results in only a 30 per cent change in rise time, and that the bulk

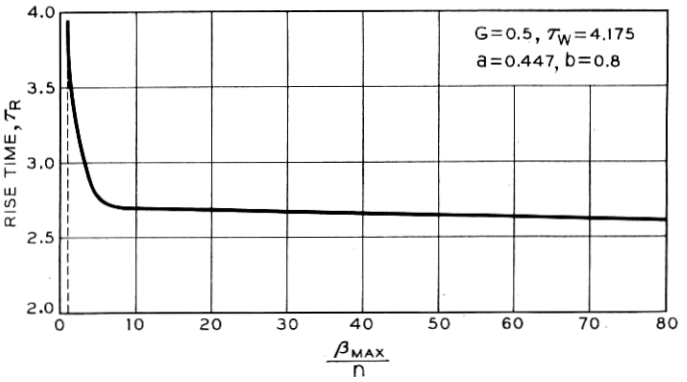

Fig. 13 — Rise time as a function of β_{max}/n.

of this change occurs for the first 7-to-1 increase in loop gain. The reason for this somewhat surprising result is, of course, the fact that the average of β/n, and therefore the average of the loop gain, is the same in all these cases.

Finally, it should also be noted in Figs. 12(a) through 12(d) that, while the rise time decreases as the slope of $f(x)$ becomes steeper, the delay increases. This is so because the collector current starts to flow much earlier in the case of a gentle slope than in the case where $f(x)$ is steep.

To investigate the effect of moving the unstable operating point, the transient response was also computed for Case 5 and Case 6 in Fig. 6. The unstable operating points in these two cases are, respectively, located in $x = 0.1$ and $x = 0.9$ and both functions have slopes identical to that of Case 3. Comparing the resulting responses of Figs. 12(e) and 12(f) with that of Fig. 12(c), it is seen that, as far as the delay and rise time are concerned, the location of the unstable operating point has even less effect than the slope has. A slightly smaller rise time is obtained when the unstable operating point is located farther away from the stable one, since the trigger is larger in such cases.

Before concluding this section, it should again be pointed out that the dependence of ω_0 on the average value of β must be taken into account when the above results are applied to actual circuits. The fact that $1/\omega_0$ and C_0 are nearly proportional to $\bar{\beta}$ [(7) and (15)] tends to override the somewhat weak dependencies discussed above. Transistors should therefore be selected for large ω_0 and small C_0 rather than a high β to obtain the best rise time. On the other hand, a high-low current β is desirable to increase the trigger sensitivity of the circuit. Finally, the

above results for a single pair of values of a and b and a single value of τ_w apply to other values of these parameters. The basic shapes of the curves in Figs. 11 and 13 remain practically unaltered. The principal effect of other values of these constants is to displace these curves both horizontally and vertically, with the vertical displacement the most pronounced effect.

6.3 *The Effect of Leakage Inductance and Collector Capacitance upon the Delay and Rise Time*

To investigate how the leakage inductance and collector capacitance affect the delay and rise time, the transient response of the blocking oscillator was computed from (35) for a large number of values of the constants a and b. Four different types of trigger signals were used throughout this investigation. In the first case, the effect of a very slow trigger signal was simulated by employing a Gaussian pulse for $g(\tau)$ of magnitude and width equal to $G = 0.3$ and $\tau_w = 166.7$, respectively. As pointed out in a previous section, this represents the case in which the rise time is solely dependent upon the properties of the feedback loop of the blocking oscillator and not upon the detailed behavior of the trigger signal itself. In the next two cases, Gaussian pulses of medium ($\tau_w = 25$) and extremely small ($\tau_w = 4.175$) widths were used, illustrating situations where both the trigger signal and the circuit properties affect the rise time. In all three cases, however, a magnitude of the trigger signals was selected such that the circuit operated on the flat portions of the curves in Fig. 11. In the fourth and last case, a step function of magnitude sufficient to saturate the transistor immediately ($G = 1$) was applied. Since the entire driving capability of the transistor is now employed from the very beginning, this represents the situation in which the delay and rise time are minimized. Also, the loop gain is zero during the entire transition, so that the degenerative effect of positive feedback on rise time is nonexistent in this case. Finally, in all cases, the blocking oscillator was assumed to be initially at rest at its stable operating point, and the analytical function in (37) was used to represent the i_c/i_b characteristic.

Figs. 14(a) through 14(d) give the delay time as a function of the constants, a and b, in the four cases. It is seen that in nearly all cases the delay is a linear function of b when either this constant or a is considerably larger than one. The only noticeable deviation from this rule is the $a = 8$ curve in Fig. 14(b), which starts to bend upwards for large b. The reason for this is that here the critical triggering level approaches the actual trigger magnitude as b is increased; in other words, the circuit is

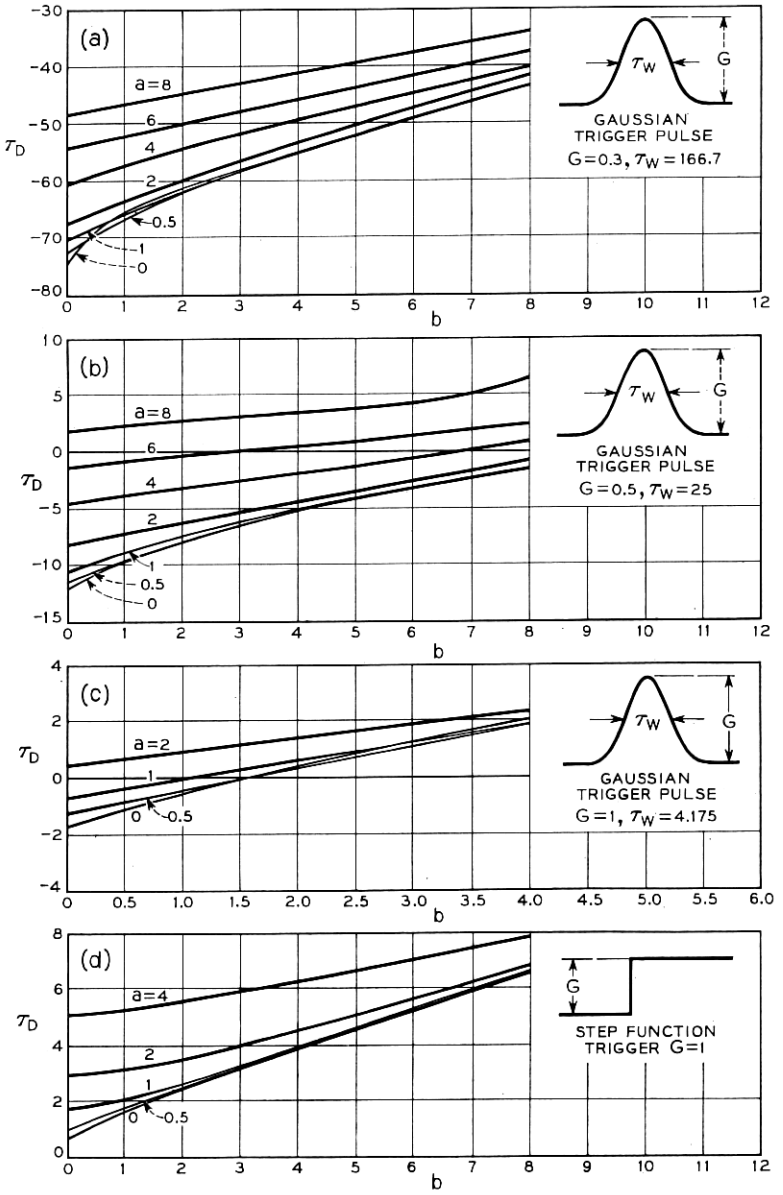

Fig. 14 — The delay as a function of a and b when the trigger signal is (a) a very slow Gaussian pulse; (b) a moderately fast Gaussian pulse; (c) a short Gaussian pulse and (d) a step function.

no longer operating on the flat portions of the curves in Fig. 11. From Fig. 14(a) it should be noted that, for values of b less than 4, the delay goes through a minimum when a is varied.

Figs. 15(a) through 15(g) show the rise time as a function of a and b for the four trigger functions. Comparing these figures, it is seen that the rise time is largest in the case of a very slow trigger signal and smallest in the case of the saturating step function. However, the variation in rise time with b is much less in the former case than in the latter one, while with a it is somewhat the other way around. Also, the dependence is stronger upon b than upon a. Finally, in all cases, the rise time goes through a minimum when a is varied and b kept fixed, this minimum being most pronounced in the case of a moderately fast trigger pulse [Fig. 15(d)].

Since it is usually not possible to obtain an analytical solution to (35), an expression for the rise time that is valid under all conditions cannot be found either. However, in two of the cases discussed above, approximate expressions for the rise time were found to fit the computed data over a limited range. The first of these pertains to the case of a very slow trigger signal and was obtained by a trial-and-error procedure. It was discovered that the expression

$$\tau_R \approx 7.85 \sqrt{1 + 2b + a} \tag{46}$$

approximates the computed data in Fig. 15(a) within ±10 per cent. The second expression for the rise time is concerned with the case where a unit step function is applied to the circuit. Since the transistor is saturated immediately in this case, (35) is linear with $f[y + g(\tau)] = 1$, and the transistor can be characterized by the transfer function

$$\frac{Y(s)}{U(s)} = \frac{1}{(s + 1)(a^2s^2 + bs + 1)}, \tag{47}$$

where $U(s)$ is the Laplace transform of the unit step function. The poles of the transfer function are given by $s = -1, -\alpha, -\beta$, where

$$\alpha = \frac{b + \sqrt{b^2 - 4a^2}}{2a^2} \quad \text{and} \quad \beta = \frac{b - \sqrt{b^2 - 4a^2}}{2a^2}. \tag{48}$$

It can be shown that a system with a transfer function whose only singularities in the finite part of the complex plane are negative real poles will have monotonic step response.[13] For the blocking oscillator, α and β are real when $b \geqq 2a$ and a monotonic step response results. Under these conditions, Elmore's definition[10] of delay and rise time gives results in good agreement with those obtained by the exact calculations

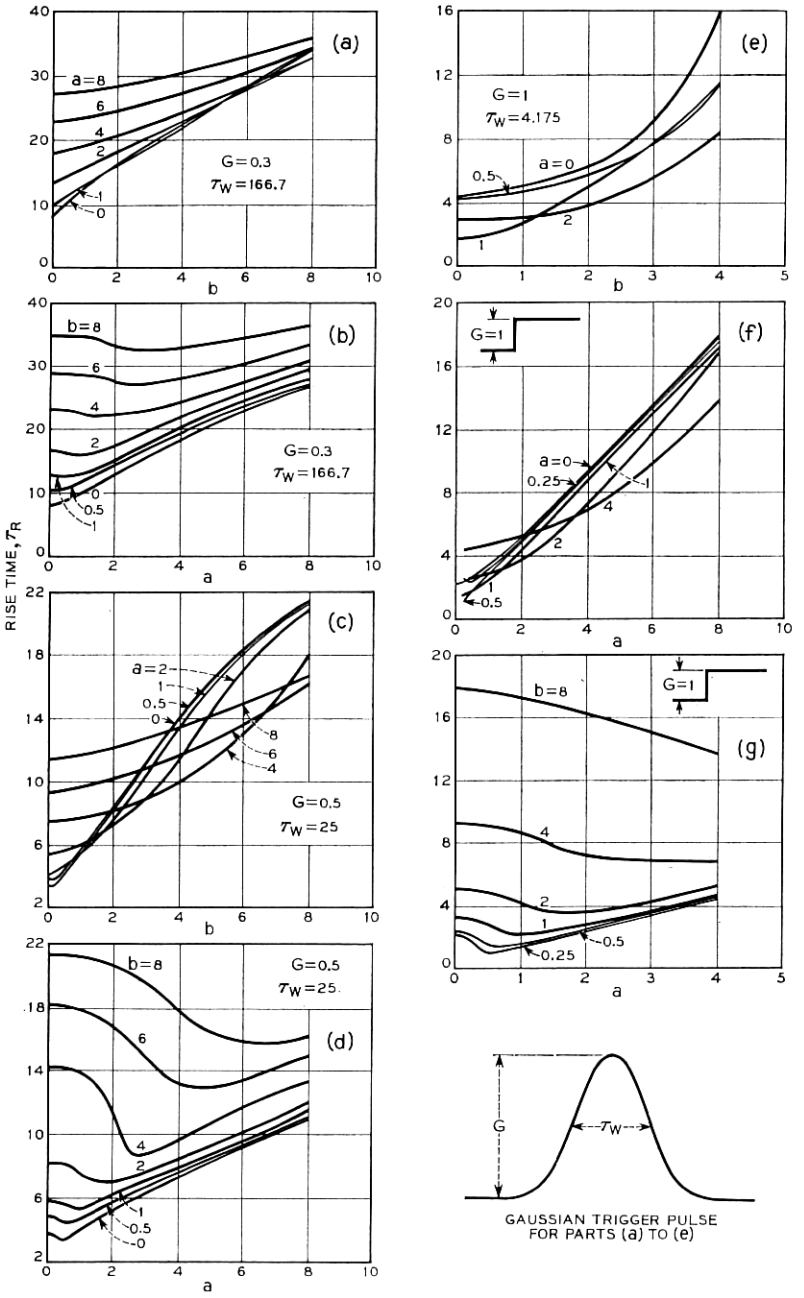

Fig. 15 — Rise time of the blocking oscillator as a function of the constants a and b when the trigger signal is: (a) and (b) a very slow Gaussian pulse; (c) and (d) a moderately fast Gaussian pulse; (e) a very short Gaussian pulse; (f) and (g) a step function of sufficient magnitude to saturate the transistor immediately.

used to obtain the results of Fig. 15. Application of Elmore's definitions yield the normalized delay

$$\tau_D = 1 + b \qquad b \geqq 2a \quad (49)$$

and the normalized rise time

$$\tau_R = 2.2\sqrt{1 + b^2 - 2a^2} \qquad b \geqq 2a \quad (50)$$

or, in unnormalized form (neglecting parasitic capacity):

$$T_D = \frac{1}{\omega_0} + R_c C_0 = (1 + n)\left(\frac{1}{\omega_\alpha} + 1.5R_c C_c\right), \quad (51)$$

$$\begin{aligned} T_R &= 2.2\sqrt{\frac{1}{\omega_0^2} + R_c^2 C_0^2 - 1.5L_e C_0} \\ &= 2.2(1 + n)\sqrt{\frac{1}{\omega_\alpha^2} + 2.25R_c^2 C_c^2 - 2.25\frac{L_e C_c}{1 + n}}. \end{aligned} \quad (52)$$

As expected, n and $R_c C_c$ should be selected as small as possible to reduce the rise time while ω_α should be large. Equation (52) suggests that there exists a value of the leakage inductance that will minimize the rise time. The exact value of the leakage inductance that accomplishes this cannot be determined from (52), since it is strictly valid only when the response is monotonic.

Finally, in Figs. 16(a) through 16(c) the overshoot is shown as a function of a, with $b/2a$ as a parameter. It is seen that, as $b/2a$ increases, the overshoot decreases, becoming zero when $b/2a \geqq 1$. It should be noted that, for fixed values of $b/2a$, the overshoot approaches a constant when a is large. Spot checks of these analog computer results were made on a digital computer, with excellent agreement between the two results.

6.4 *Conditions for Monotonic Response*

In the preceding section it has been shown that the blocking oscillator will have monotonic or oscillatory response when it is driven by a saturating step function, depending on whether b is greater than or less than $2a$ respectively. For example, the response will be monotonic if

$$b > 2a \qquad \text{or} \qquad R_c > 2\sqrt{\frac{L_e}{C_0}}, \quad (53)$$

and be oscillatory if

$$b < 2a \qquad \text{or} \qquad R_c < 2\sqrt{\frac{L_e}{C_0}}. \quad (54)$$

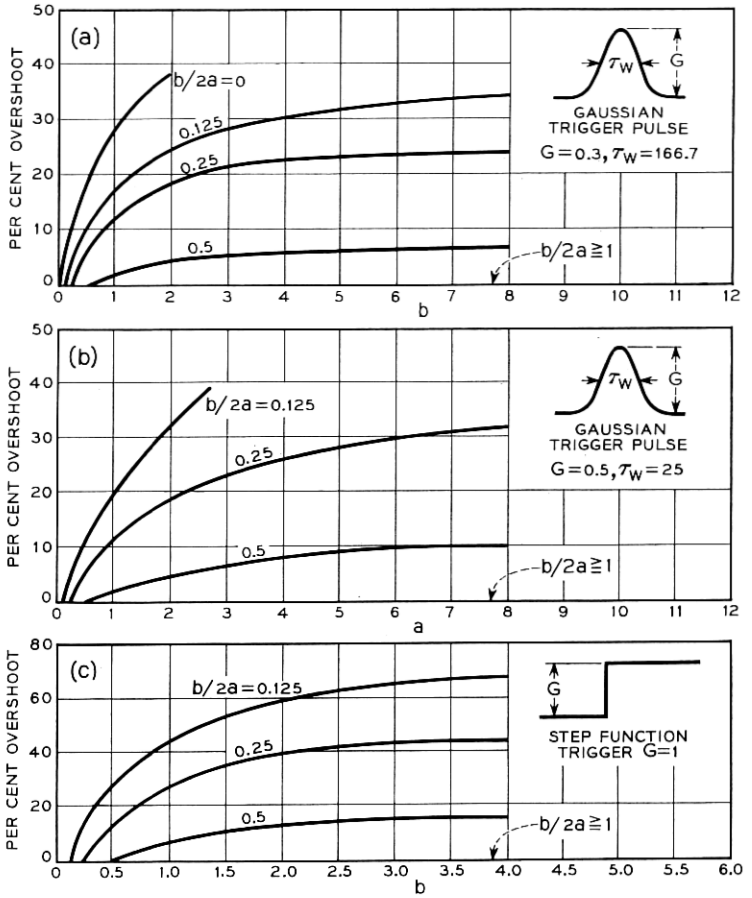

Fig. 16 — The percentage overshoot of the blocking oscillator when the trigger signal is (a) a very slow Gaussian pulse; (b) a moderately fast Gaussian pulse and (c) a step function.

The condition $b = 2a$ yields two coincident real roots and divides the a–b plane into regions of monotonic and oscillatory responses, as shown in Fig. 17. Two real roots can also result when either α or β is equal to -1. This leads to the parabola

$$b = 1 + a^2 \tag{55}$$

in the a–b plane. At the point (1, 2) this parabola is tangent to the straight line $b = 2a$ and the blocking oscillator has three coincident real poles at $s = -1$.

There is one exception to the above division in the a–b plane. When $b = 2a^2$ and $0 < a < 1$, a pair of complex conjugate poles whose real part $= -1$ arises. The poles all lie on a line that is parallel to the imaginary axis in the complex plane and spaced one unit to the left. In this case, the impulse response is tangent to the zero line, so that the step response is monotonic. It can be shown that in the region $b \geqq 2a^2$, $0 \leqq a \leqq 1$ the response will be monotonic. The rise time in this case with $b = 2a^2$ is given by

$$\tau_r = 2.2\sqrt{1 + 4a^4 - 2a^2}\,. \tag{56}$$

The above rise time is a minimum when $a = 0.5$; the minimum rise time then is 1.87. Actual transient calculations for this condition yield a minimum rise time of 1.45 at $a = 0.45$. In this case, the 10 to 90 per cent rise time is faster than it is in any of the other cases of monotonic response. However, the response proceeds quite slowly from the 90 per cent point to its final unit asymptote. This behavior explains the discrepancy between the results of (56) and the exact transient calculations.

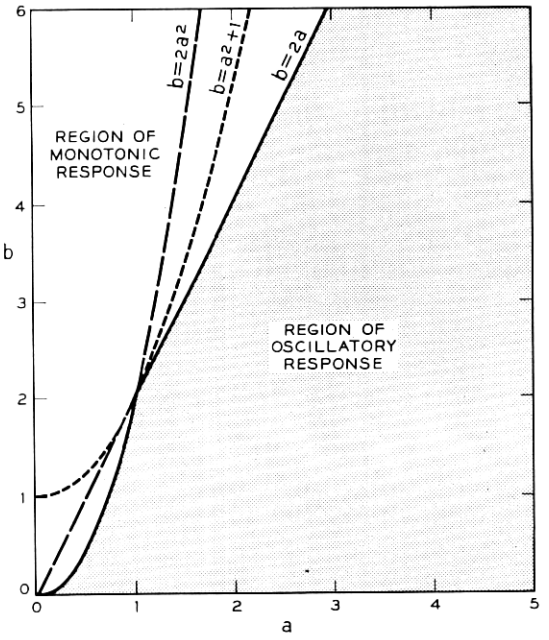

Fig. 17 — Conditions for monotonic step response.

Ideally, the blocking oscillator should have a response that has both as small a rise time as possible and a flat, smooth top. The best physical compromise to this requirement is to make the circuit nearly critically damped during this interval. In other words, the coefficients a and b should be selected such that they lie in a region close to the straight line, $b = 2a$, in Fig. 17, i.e.,

$$b \doteq 2a \qquad \text{or} \qquad R_c \doteq 2\sqrt{\frac{L_e}{C_0}}. \tag{57}$$

Furthermore, Figs. 15(f) and 15(g) show that a minimum rise time can be achieved for small values of a and b. In fact, a rise time faster than the minimum rise time of the transistor itself ($2.2/\omega_0$) can be obtained. Some overshoot is associated with these cases. This result is similar to that achieved with series peaking in a conventional interstage, and confirms the conclusions of Linvill and Mattson.[3] However, in this case the blocking oscillator is acting as an overdriven amplifier with zero loop gain. The larger the drive the faster the response, since ω_0 increases with drive. Smallest rise time can only occur when the power gain required of the blocking oscillator is low. This requirement may be satisfied in some computer applications where the primary function of the blocking oscillator is to retime a relatively sharp pulse train. In applications where the blocking oscillator must reshape as well as retime a pulse train, such as in pulse code modulation, considerable power gain will be demanded from the circuit and the minimum rise time cannot be achieved. This is the analog of the familiar gain-bandwidth product for linear systems.

When signals other than the saturating step function are used to trigger the blocking oscillator, the manner in which the quasistable operating point is approached is dependent on the parameters a and b, the nonlinear characteristic and the trigger signal. When the transistor saturates after suitable triggering $f[y + g(\tau)] = 1$. At this point, as noted previously, (35) is linear and the Laplace transform of the output can be expressed as:

$$y(s) = \frac{1}{s[a^2s^3 + (a^2 + b)s^2 + (1 + b)s + 1]} + \tag{57}$$

$$\frac{[a^2s^2 + (a^2 + b)s + (1 + b)]y(t_s) + [a^2s + (a^2 + b)]y'(t_s) + a^2y''(t_s)}{a^2s^3 + (a^2 + b)s^2 + (1 + b)s + 1},$$

where $y(t_s)$, $y'(t_s)$ and $y''(t_s)$ are, respectively, the values that y, its first and its second derivatives attain when the transistor becomes

saturated. The kind of response $y(t)$ will have is therefore dependent upon both the initial conditions at saturation and the roots of the characteristic equation

$$a^2s^3 + (a^2 + b)s^2 + (1 + b)s + 1 = (s + 1)(a^2s^2 + bs + 1) = 0. \tag{58}$$

Relationships between the initial conditions and a and b can be established such that the quasistable operating point is approached monotonically.[13] This will not be pursued here, since the values of the derivatives at saturation are not normally measured quantities. On purely physical grounds, it would be expected that the conditions given previously for monotonic response in the case of the saturating step function should also apply here. This follows when it is realized that the saturating step function brings the full capability of the transistor into play immediately, thereby imparting maximum energy into the output circuit. For other trigger signals this will not be true, so that the energy transferred to the output circuit will be smaller than it will be in the case of the saturating step. Since the values of the output function and its derivatives when the transistor goes into saturation are a measure of this energy, it would appear that, if no overshoot occurs with the saturating step, none should occur for other trigger signals. This heuristic argument is bolstered by the results displayed in Figs. 18(a) and 18(b). These figures give the analog computer solutions to (35) for various values of a and b when either a fast or slow trigger is applied to the circuit. In both cases the response adheres to the conditions given on Fig. 17 for monotonic response.

VII. THE "ON" INTERVAL

After the blocking oscillator has reached the quasistable operating point the magnetizing inductance becomes charged slowly, reducing the current fed back to the base. This causes the load line, and therefore the quasistable operating point, to move to the left, in Fig. 4 or 5, until the load line is tangential to the $I(i_b)$ curve. Beyond this point (J′), the load line intersects $I(i_b)$ only in the cutoff region, and the circuit now has only one possible operating point. Hence, a rapid "jump" toward cutoff takes place at J′, and it is therefore natural to define the "On" interval as the time it takes the base current to decrease from the quasistable operating point to the value it has at the point of tangency, J′, that is:

$$I_{bj} \leqq i_b \leqq I_{bs} \tag{59}$$

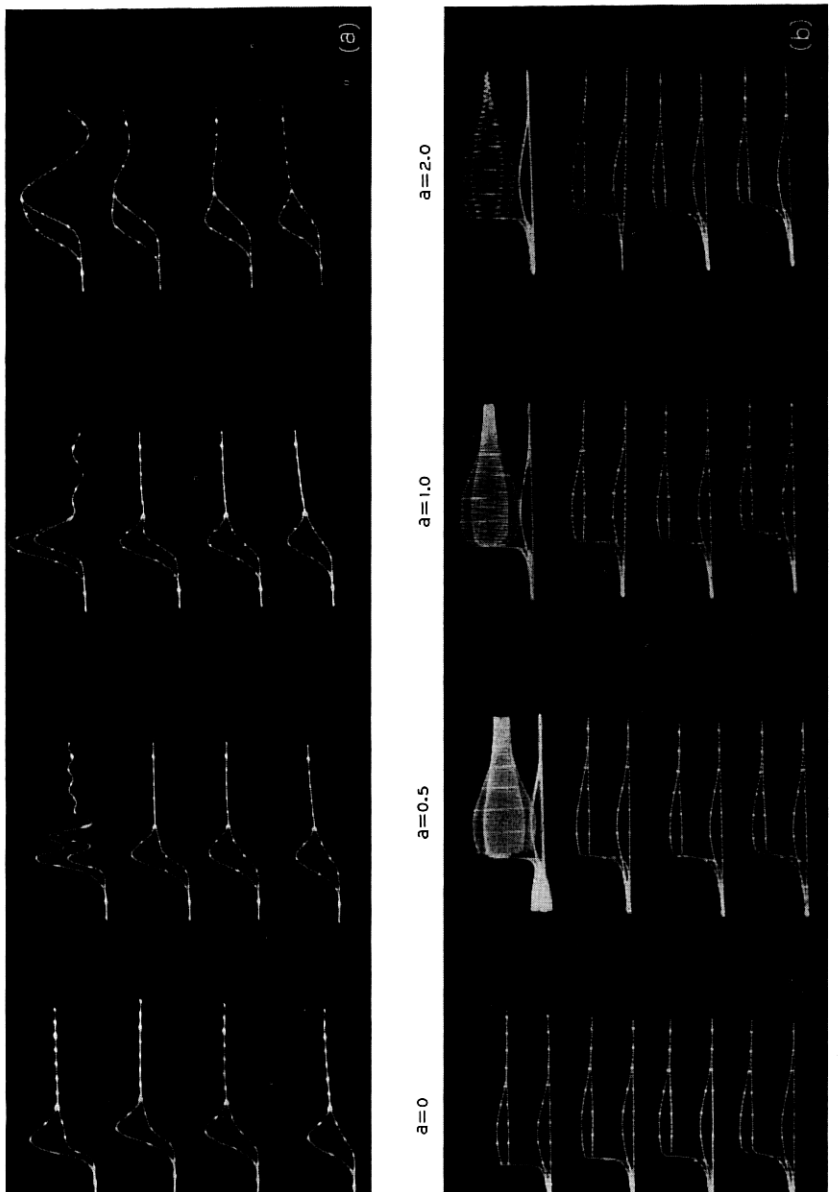

Fig. 18 — (a) Transient responses when $G = 1$ and $T_w = 4.175$, with the upper curves being base current, x, and the lower curves output voltage, y; (b) transient responses when $G = 0.3$ and $T_w = 160$, with the upper curves being base current, x, the middle curves output voltage, y, and the lower curves the trigger function.

In Fig. 19 the results of solving the complete equation [(116) of Appendix B] of the blocking oscillator on an analog computer are shown. The analytical representation (37) of the i_c/i_b characteristic was used and $V(x)$ was approximated by two straight-line segments. Also, the constants a, b, d and e were kept fixed while the constant c, which is proportional to the magnetizing inductance, was varied. It is seen that, except when c is small and the circuit oscillates, the base current and the base voltage vary rather slowly during the "On" interval. Hence, during this interval terms involving derivatives of x and $V(x)$ may be neglected. This also follows from the fact that, in all cases of practical interest, the magnetizing inductance is very large compared with the other storage elements in the circuit. For the same reason, the amount of current collected by this inductance during the "Transition On" interval is also assumed to be negligible, i.e., $m(\tau_j) \doteq 0$. Assuming the trigger signal to have terminated by this time, the equation governing the normalized base current during this interval therefore reduces to

$$x - h(x) + \frac{1}{c}\int_0^\tau V(x)\,d\tau = 0$$

or

$$c\frac{dx}{d\tau} + \frac{V(x)}{1 - \dfrac{dh(x)}{dx}} = 0. \tag{60}$$

The unnormalized version of this equation becomes

$$n^2 L_m \frac{di_b}{dt} + \frac{V_b(i_b) - E_{bb}}{1 - \dfrac{dI(i_b)}{di_b}} = 0. \tag{61}$$

The above equation reflects the operation of the circuit during this interval exactly as it was described at the beginning of this section. First, it indicates that the base current decreases rather slowly, since L_m is large and $V_b(i_b) - E_{bb}$ small. Then, when $dI(i_b)/di_b$ becomes equal to unity [which corresponds to the point of tangency (J′) in Fig. 4], it predicts that a jump takes place, by virtue of the fact that $di_b/dt = \infty$ at this point. Since

$$1 - \frac{dI(i_b)}{di_b} = \frac{R_b' + \dfrac{dV_b(i_b)}{di_b}}{R_b'}\left[1 - \frac{1}{n}\frac{R_b'}{R_b' + \dfrac{dV_b(i_b)}{di_b}}\frac{dI_c(i_b)}{di_b}\right], \tag{62}$$

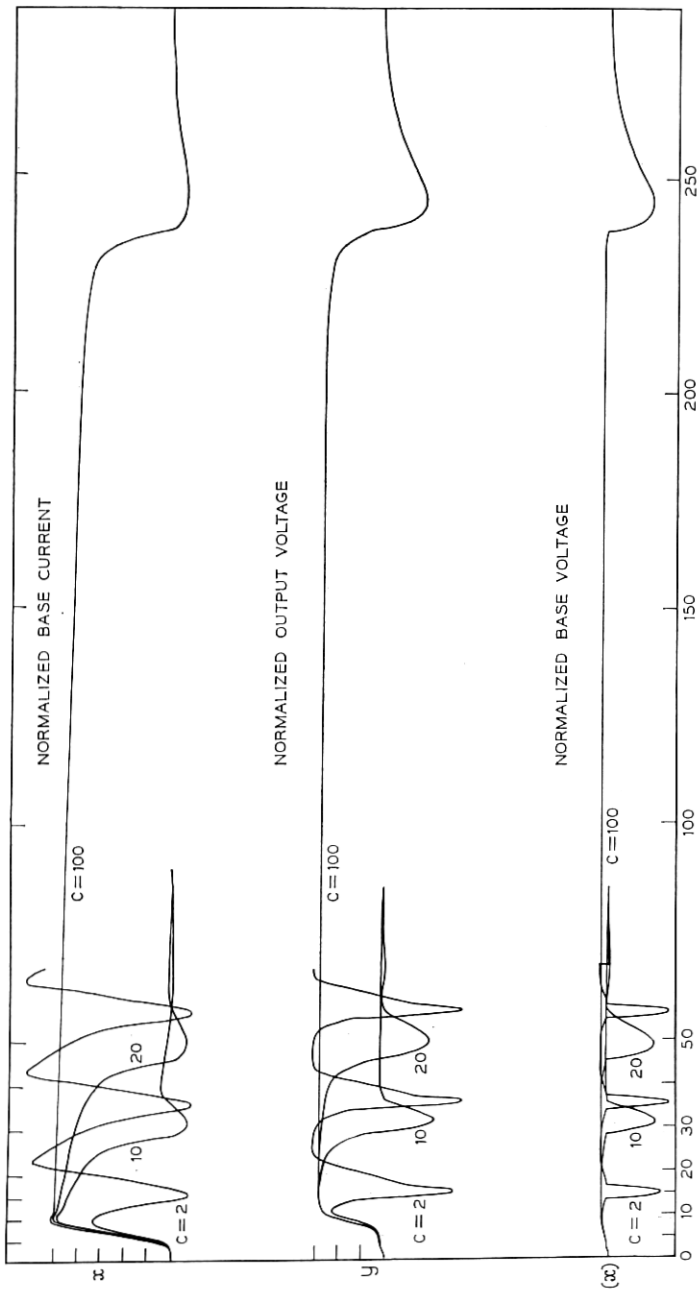

Fig. 19 — Natural pulse width of the blocking oscillator when c = 2, 10, 20 and 100. An analytical $f(x)$ was used and a^2 = 0.2, b = 0.8, d = 0.28, G = 0.5 and τ_w = 4.175.

it can be seen that the "midband" loop gain of the circuit is equal to unity at the point where the jump takes place.

As a first step toward deriving a formula for the natural pulse width of the blocking oscillator, let us introduce the above expression into (61) and also take advantage of the fact that $V_b(i_b)$ is very nearly linear in the saturation region, so that $V_b(i_b) = r_{bs}i_b$. Thus, (61) becomes:

$$n^2L_m \frac{R_b' + r_{bs}}{R_b'r_{bs}} \frac{di_b}{dt} + \frac{i_b - \dfrac{E_{bb}}{r_{bs}}}{1 - \dfrac{1}{n}\dfrac{R_b'}{R_b' + r_{bs}}\dfrac{dI_c(i_b)}{di_b}} = 0. \tag{63}$$

By substituting the analytical approximation for $I_c(i_b)$, the above equation may be solved exactly.[14] However, in cases of practical interest, the quasistable operating point extends quite far into the saturation region and, furthermore, most i_c/i_b characteristics bend quite sharply before going into saturation. Therefore the jump point, J', is positioned very close to the saturation level. Hence, the transistor is saturated during almost the entire "On" interval with the result that $dI_c(i_b)/di_b$ is equal to zero except in the near vicinity of the point J'. For the purpose of deriving an expression for the pulse width, it is therefore an excellent approximation to neglect the loop gain term in (63). Solving this equation under these conditions, introducing i_b as equal to I_{bs} and I_{bj} at the beginning and end of the "On" interval and substituting for R_b' from (24), the expression for the natural pulse width may be written

$$T_w \sim n^2L_m \frac{R_b + r_{bs}\left[1 + \dfrac{R_b}{n^2L_m}\left(\dfrac{1}{\omega_0} + R_cC_0\right)\right]}{R_br_{bs}} \ln \frac{I_{bs} - \dfrac{E_{bb}}{r_{bs}}}{I_{bj} - \dfrac{E_{bb}}{r_{bs}}}. \tag{64}$$

In most circuits

$$R_b \gg r_{bs}\left[1 + \frac{R_b}{n^2L_m}\left(\frac{1}{\omega_0} + R_cC_0\right)\right] \quad \text{and} \quad I_{bs} \doteq \frac{I_{cs}}{n}, \tag{65}$$

so the above equation reduces to

$$\frac{T_w}{L_m/r_{bs}} \doteq n^2 \ln \frac{\dfrac{1}{n} - \dfrac{E_{bb}}{I_{cs}r_{bs}}}{\dfrac{I_{bj}}{I_{cs}} - \dfrac{E_{bb}}{I_{cs}r_{bs}}}. \tag{66}$$

Figs. 20 and 21 show the normalized pulse width as a function of n for various values of I_{bj}/I_{cs} and $E_{bb}/I_{cs}r_{bs}$ as computed from (66). It is seen

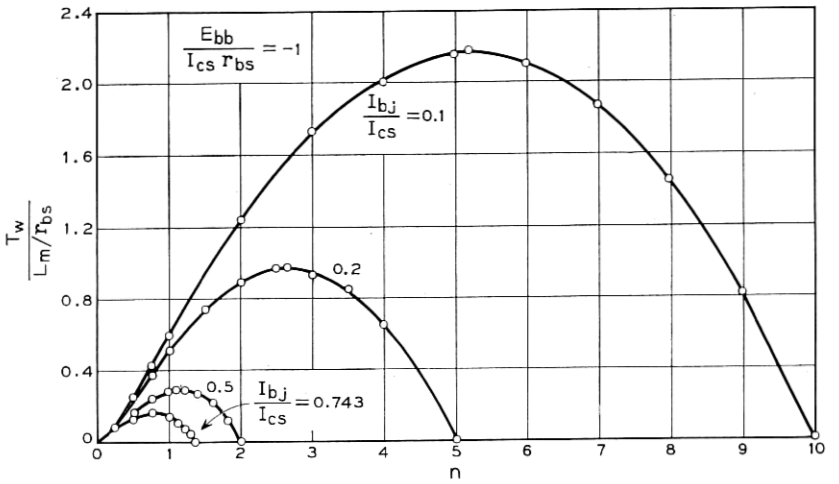

Fig. 20 — Pulse width as a function of turns ratio, with $E_{bb}/I_{cs}r_{bs} = -1$.

that the pulse width goes through a maximum and is nonzero over only a finite range of n, the limiting values of n being 0 and I_{cs}/I_{bj}. Physically, the upper limit corresponds to the coincidence of the quasistable and the unity loop gain points, making it impossible for the circuit to remain in a conducting state for a finite time. It should be noted from these figures that, for a fixed turns ratio, the natural pulse width exhibits a strong dependence upon both $E_{bb}/I_{cs}r_{bs}$ and I_{cs}/I_{bj}, i.e., on both the nonlinearities and the bias.

Before concluding this section, two things should be pointed out. First, the quantity I_{bj} in (66) is, strictly speaking, also a function of n, because, as n is varied, the point of tangency in Fig. 4 changes. However, since the i_c/i_b characteristic usually bends quite sharply before going into saturation, I_{bj} will vary only slightly with n. Second, in the above analysis the effect of minority carrier storage has been neglected. The presence of such carriers in the collector junction introduces a delay before the transistor can leave the saturation region; as if the $I(i_b)$ curve had been temporarily moved somewhat to the left in Fig. 4, thereby causing the pulse width to be slightly larger than that predicted by (60). However, this effect may be partially accounted for by calculating the pulse width from (64) rather than from (66), using, as explained in the section on the equivalent circuit, the value of ω_0 appropriate to turnoff.

VIII. THE "TRANSITION OFF" INTERVAL

In discussing the "Transition Off" interval one must discriminate between two cases: one in which the blocking oscillator turns off by

itself, and the other when it is triggered off by virtue of an externally applied signal. In the following, these two cases will be discussed separately.

8.1 *Internal "Turn Off"*

As explained in the previous section, when the magnetizing inductance becomes sufficiently charged so that the load line is tangent to the $I(i_b)$ curve at the unity loop gain point, J′, a rapid transition toward the other point of intersection between the load line and the characteristic takes place. Since the input impedance to the transistor is very high in the reverse direction, the bias current, I_{bc}, is very small and the $I(i_b)$ curve is almost vertical in the cutoff region. Thus, the end point of the transition is essentially located on the $i_b = 0$ axis. Hence, it is natural in this case to define the "Transition Off" interval as the time it takes the base current to vary between I_{bj} and $I_{bc} \doteq 0$. The transistor is therefore conducting over almost this entire interval and the same approximations can be made here as for the "Transition On" interval. Accordingly, the equations governing the responses in the two intervals will be alike, the only differences being that the trigger signal is absent and the magnetizing current is

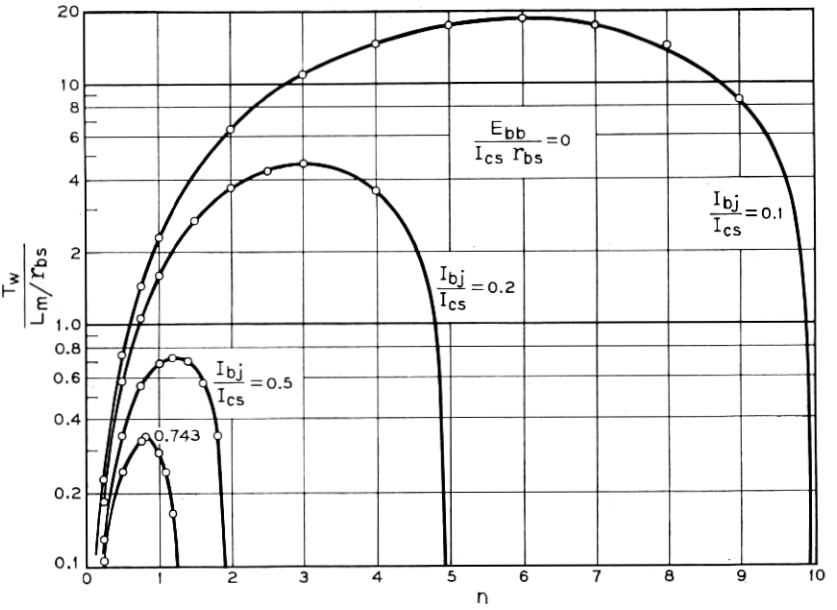

Fig. 21 — Pulse width as a function of turns ratio, with $E_{bb}/I_{cs}r_{bs} = 0$.

$$I_m(t_j) = I_c(I_{bj}) - n\left\{\left[1+\frac{R_b}{n^2L_m}\left(\frac{1}{\omega_0}+R_cC_0\right)\right]\frac{V_b(I_{bj})-E_{bb}}{R_b}+I_{bj}\right\} \quad (67)$$

$$\doteq I_c(I_{bj}) - nI_{bj}$$

or, in normalized form,

$$m(\tau_j) = f(x_j) - \left(1+\frac{1+b}{c}\right)V(x_j) - x_j \doteq f(x_j) - x_j. \quad (68)$$

As explained in the section on the equivalent circuit, a different ω_0 that takes into account the effect of minority carrier storage must now be used. This latter modification usually results in a fall time that is from two to ten times that of the rise time.

The fall time in this case may be calculated in an alternate way which permits one to use the results in Section IV. The accumulation of current in the magnetizing inductance acts like a slowly varying bias that slides the load line toward the point of tangency, at which point rapid regeneration takes place. This fact suggests that the mode of operation now is very similar to the case in which a slow trigger signal is applied to the circuit. Hence, if one defines the fall time as the time taken for the response to traverse 90 to 10 per cent of the interval between the stable and quasistable operating points, one should expect that the fall time can be obtained directly from Fig. 15(a) or (46), provided the ω_0 valid in this interval is used. Indeed, comparisons of rise and fall times between Figs. 15(a) and 19 bear this out.

8.2 *External "Turn Off"*

When the blocking oscillator is turned off by an external signal the natural pulse width is always selected to be much larger than the interval between the "Turn On" and the "Turn Off" pulses, in order to secure reliable operation. The magnetizing inductance will therefore not become significantly charged during the time the circuit is on and conditions similar to those during the "Transition On" interval exist. By using the value ω_0, which takes into account the effect of minority carrier storage, the fall time in this case may be calculated from the results in Section IV.

IX. THE "RECOVERY" INTERVAL

This interval is defined as the difference in time between cutoff and the time the circuit comes to rest at the stable operating point. During this interval, assuming that the recovery is overdamped or slightly

oscillatory, it is reasonable to assume that the transistor is essentially cut off. This means that the β of the transistor is zero, $f(x)$ is essentially zero and C_0 reduces to

$$C_0 = C_c + C_s . \tag{69}$$

In addition, the terms involving the normalized base voltage will be considerably larger than those containing the normalized base current in the complete equation governing the circuit operation. Since the terms containing derivatives of the normalized base voltage are unimportant in the preceding operating intervals, their coefficients can be modified in terms of the values they assume during recovery without affecting performance in the other intervals. In this case, we do not operate on the base voltage terms with the expression

$$\left(1 + \frac{1}{\omega_0}\frac{d}{dt}\right) i_c = I_c(i_b), \tag{70}$$

since the transistor, except for its output capacity C_c, is effectively disconnected from the output circuit while it rings out. In addition, the parameter e which arises from the capacity across the transformer is lumped in with the constant d, to give a value of d modified to

$$d_1 = \frac{\omega_0 R_b}{n^2}\left[(C_c + C_s)\left(1 + \frac{L_e}{L_m}\right) + C_T\right]. \tag{71}$$

Finally, derivatives of v_b higher than the second were neglected. With this reasoning, the terms that remain involving $V(x)$ in the normalized equation of the blocking oscillator are

$$(a_1^2 + be)\frac{d^2V}{d\tau^2} + (b + d_1)\frac{dV}{dt} + \left(1 + \frac{b}{c}\right)V + \frac{1}{c}\int_{\tau_j}^{\tau} V\, d\tau, \tag{72}$$

where

$$\left.\begin{aligned} a_1 &= a \\ b_1 &= b \end{aligned}\right\} \quad \text{with} \quad C_0 = C_c + C_s . \tag{73}$$

With this change, the equation governing the performance of the blocking oscillator over its complete cycle of operation was simulated on an analog computer to verify the contention that the transistor is cut off during recovery, and to give quantitative substance to the assumption that only the $V(x)$ terms need be considered. Again, the analytical function was used to represent the i_c–i_b characteristic, while the normalized base voltage function was approximated by two straight line segments.

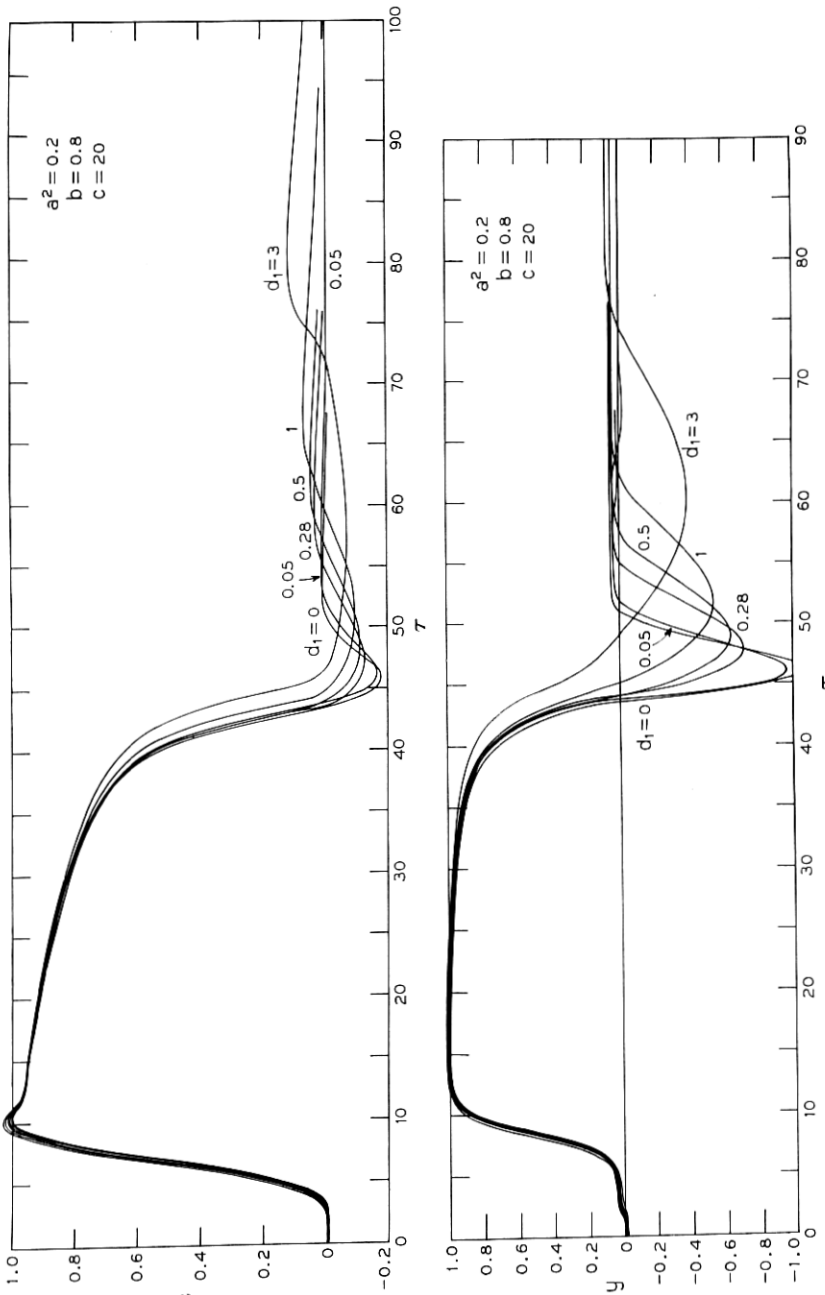

Fig. 22 — Response of the blocking oscillator for various values of d.

The circuit was turned on by a Gaussian trigger pulse of width $\tau_w = 4.175$ and magnitude $G = 0.5$, and left to its own devices to turn off. The computer results when the constant d_1 was varied and the remaining constants fixed are shown in Fig. 22. The main effect of varying d_1 is to change the response after the blocking oscillator has turned off. Recovery is rather slow, and decreases as d is increased. It should be noted that, as long as d is not too large, the overshoot of the base current is small, confirming the assumption that the transistor remains essentially cut off during recovery. The undershoot of the output voltage is rather large, becoming larger and narrower as d_1 is increased. This is largely due to the fact that the transformer capacity has been assumed negligible compared to C_0 (i.e., $e \doteq 0$). When e is greater than C_0, it will be found that the undershoot of the output voltage is quite small. This will be discussed more fully in a succeeding paragraph. From Fig. 19 it can be seen that recovery is very much dependent on the parameter c. This would be expected physically since c is associated with the energy stored in the magnetizing inductance.

From the above results it can be seen that the transistor is essentially cut off during recovery and that the base-emitter junction of the transistor is back-biased, assuring that $V(x) \gg x$. Therefore, all the assumptions of the beginning of this section are valid and the equation governing recovery can be written from the Appendix and (72) as

$$(a_1^2 + b_1 e)\frac{d^2V}{d\tau^2} + (b_1 + d + e)\frac{dV}{d\tau} + \left(1 + \frac{b_1}{c}\right)V + \frac{1}{c}\int_{\tau_j}^{\tau} V\, d\tau + m(\tau_j) = \left(1 + b_1\frac{d}{d\tau} + a_1^2\frac{d^2}{d\tau^2}\right)g(\tau). \tag{74}$$

If we differentiate (74) we get, after some rearranging,

$$c(a_1^2 + b_1 e)\frac{d^3V}{d\tau^3} + c(b_1 + d + e)\frac{d^2V}{d\tau^2} + (b_1 + c)\frac{dV}{d\tau} + V = c\left(\frac{d}{d\tau} + b_1\frac{d^2}{d\tau^2} + a^2\frac{d^3}{d\tau^3}\right)g(\tau). \tag{75}$$

Whether the response of (75) is monotonic or not depends upon the initial conditions when the recovery interval is entered, as well as the parameters a through e. In the absence of information concerning the initial conditions, we can only determine whether or not the response will be nonoscillatory. This can be determined by using the discriminant for the cubic on the homogeneous equation. Instead, we assume that the third derivative term can be neglected and deal with the second-or-

der equation in V. This approximation appears to be justified in practice. In this case, it is readily shown that the recovery response will be non-oscillatory if

$$d + e \leqq \frac{(b + c)^2}{4c} - b = \frac{(c - b)^2}{4c} \doteq \frac{c}{4}. \tag{76}$$

In unnormalized form, this becomes

$$R_b \leqq \frac{n^2 L_m}{R_c(C_c + C_s) + 2\sqrt{L_m C_T + L_m(C_c + C_s)\left(1 + \frac{L_e}{L_m}\right)}} \doteq \frac{n^2}{2}\left(\frac{L_m}{C_c + C_s + C_T}\right)^{1/2}. \tag{77}$$

During this interval, the output voltage is given by

$$y = x + e\frac{dV}{d\tau} + \frac{1}{c}\int_{\tau_j}^{\tau} V\, d\tau + V + m(\tau_j) - g(\tau). \tag{78}$$

When the transformer capacity (directly proportional to e) is much larger than $C_c + C_s$, and the derivative terms of $g(\tau)$ and the highest derivative of V are neglected, (74) becomes

$$e\frac{dV}{d\tau} + V + \frac{1}{c}\int_{\tau_j}^{\tau} V\, d\tau + m(\tau_j) - g(\tau) \doteq 0. \tag{79}$$

Comparing (79) and (78), it can be seen that they are identical when $x = 0 = y$. During recovery, x is small compared to V. The fact that $y \doteq 0$ implies that the output voltage is essentially zero during recovery when the transformer capacity $C_T \gg C_c + C_s$. This must be so from physical considerations, since the current through the load must of necessity be small when the output impedance of the transistor becomes quite high.

X. MULTIPULSE RESPONSE OF THE BLOCKING OSCILLATOR

To investigate how the blocking oscillator should be designed in order to work reliably as a regenerator in a PCM repeater, (116) of Appendix B was solved on an analog computer with $g(\tau)$ consisting of a sequence of alternating positive and negative Gaussian pulses. Each "Turn On" and "Turn Off" trigger pulse was spaced 15 time units apart, and the magnitude and width of these were $G = 0.5$ and $\tau_w = 4.175$, respectively. The analytical expression (37) was again used to represent the i_c/i_b characteristic and $V(x)$ was approximated by two straight line segments. The constants a and b were selected such that the rise time of the circuit was small

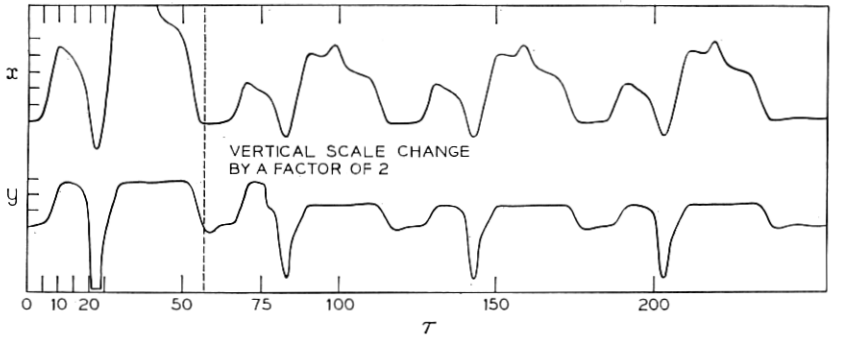

Fig. 23 — Response of the blocking oscillator to a sequence of "Turn On" and "Turn Off" pulses when $a^2 = 0.2$, $b = 0.8$, $c = 5$ and $d = 0.28$. This value of c corresponds to a natural pulse width of $\tau_w = 10$. Each "Turn On" and "Turn Off" pulse was spaced 15 units apart and had a magnitude and width of $G = 0.5$ and $\tau_w = 4.175$. The maximum of the first "On" pulse occurs when $\tau = 7.5$.

compared to the spacing between the trigger pulses and d was picked such that the recovery was reasonably fast. Finally, it was assumed that the blocking oscillator was initially at rest at the stable operating point so that $m(0) = 0$.

The results are shown in Figs. 23 through 26 for various values of the constant c; that is, the natural pulse width of the circuit was altered in these cases. In Fig. 23 the pulse width was equal to 10, and therefore it was less than half the period of the trigger signal. It is seen that, not only do the height and width of the output pulses vary considerably, but the timing information contained in the trigger signal is almost completely destroyed as well. In Fig. 24, in which the natural width

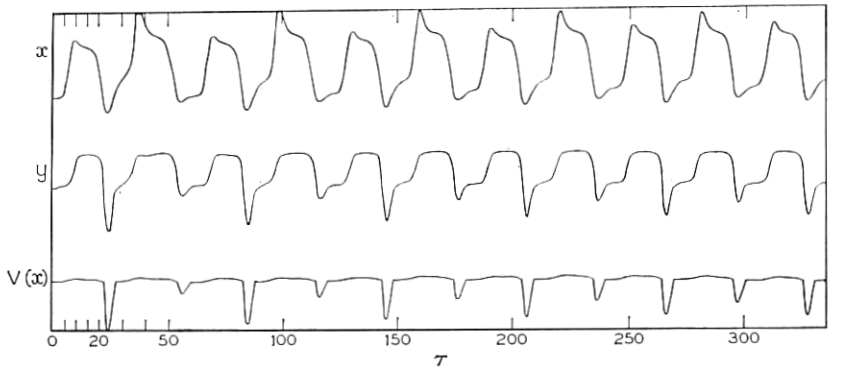

Fig. 24 — Response of the blocking oscillator to a sequence of "Turn On" and "Turn Off" pulses when $c = 10$.

was almost doubled, conditions have improved considerably. However, variations in width and timing are still intolerable. By increasing the width further by almost 40 per cent, as shown in Fig. 25, the result becomes acceptable, although the undershoot of y varies considerably. Finally, in Fig. 26, where the natural pulse width is about 1.4 times the period of the trigger on signal, the train of output pulses is almost completely uniform, with scarcely any change from one pulse to another. Hence, for the blocking oscillator to perform reliably as a regenerator, its natural pulse width should be at least equal to 1.5 times the repetition period or equivalent, three times the time interval, T_T, between each "Turn On" and "Turn Off" pulse for a 50 per cent duty cycle; that is,

$$T_w \geqq 3T_T \tag{80}$$

In addition, the rise time should, of course, be considerably less than T_T and the recovery should be such that it is overdamped or only slightly oscillatory.

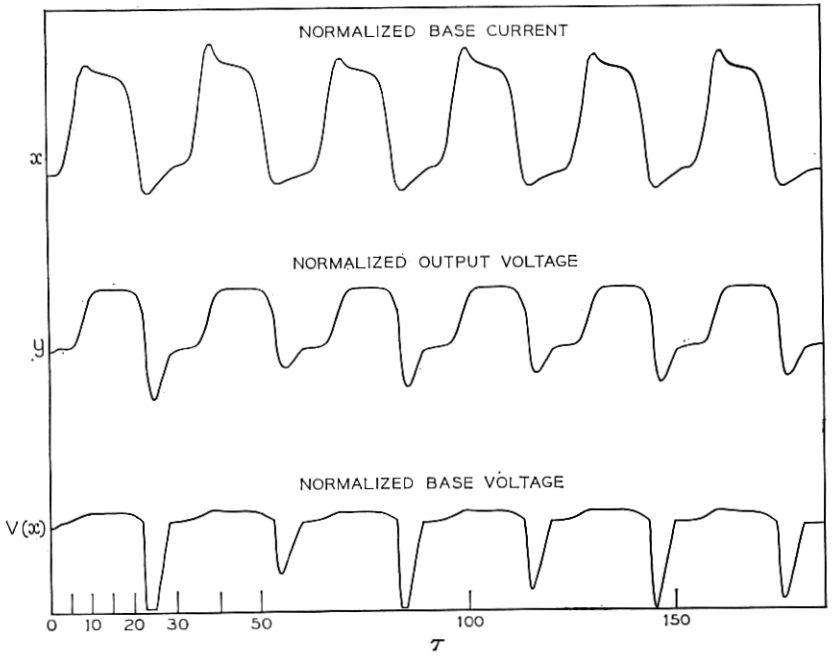

Fig. 25 — Response of the blocking oscillator to a sequence of "Turn On" and "Turn Off" pulses when $c = 14.3$.

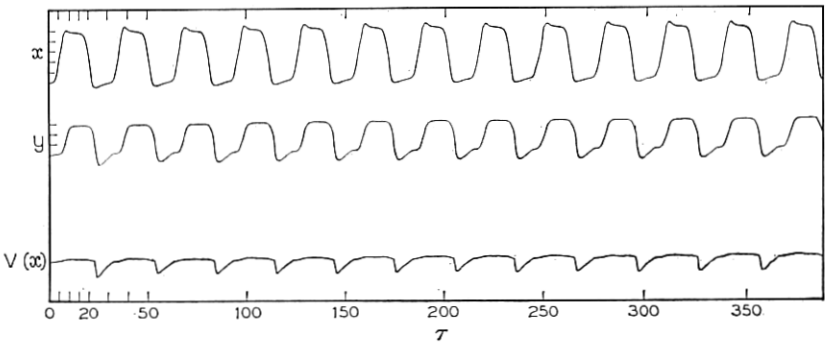

Fig. 26 — Response of the blocking oscillator to a sequence of 13 "Turn On" and "Turn Off" pulses when $c = 25$. This value of c corresponds to a natural pulse width for the circuit of $\tau_w = 41.5$.

Physically, the above results are what one should qualitatively expect. When the natural width is about equal to or less than T_T, the turnoff mechanism in the blocking oscillator itself will interfere with the trigger signal, while in the case of a large width the circuit works more or less like a bi-stable device, thus reproducing the incoming signal faithfully.

XI. DESIGN EXAMPLE

To illustrate how the results of the foregoing discussion may be used to develop a design procedure for the blocking oscillator, let us consider the following typical problem.

A grounded emitter blocking oscillator is to be used as a pulse regenerator working at a maximum repetition rate of 1.5 mc. It should be triggered "on" and "off" by a circuit having an output impedance of $R_b = 1000$ ohms and it must work into a load of $R_c = 400$ ohms. The available bias voltages for the base and collector circuits are $E_{bb} = -0.8$ volt and $E_{cc} = -6$ volts, respectively, and the stray and wiring capacity was estimated to be about 5 micromicrofarads. Available transformers for this application have parameters referred to the primary in the neighborhood of the following:

Leakage inductance: $L_e \doteq 1$ μh,

Magnetizing inductance: $L_m \doteq 100$ μh,

Stray capacitance: $C_T \doteq 20$ $\mu\mu$f,

Possible turns ratios: $n = 1.5, 3, 4.5$.

A surface barrier transistor, 2N128, is to be used, for which typical

$I_c(i_b)$ and $[V_b(i_b) - E_{bb}]/R_b$ characteristics are shown in Fig. 27(a). Its other specifications are as follows:

Collector saturation current with R_c = 400-ohm load: I_{cs} = 14.5 ma,

Minimum base current to saturate transistor: $I_{bs\ \min}$ = 2 ma,

Base voltage at the point of saturation: $\doteq$ 0.5 volt,

Base input impedance in the conduction region: r_{bs} = 60 ohms,

α cutoff frequency: f_α = 60 mc,

Collector capacitance: C_c = 1.6 $\mu\mu$f,

$\beta_{\max}$ = 37.

The "Turn On" and "Turn Off" trigger pulses have roughly a Gaussian shape and are spaced 0.33 microsecond apart. Their 50 per cent width is about 0.2 microsecond and their magnitude should be determined. The rise time and fall time of the blocking oscillator should be less than 0.15 microsecond.

The first step to be taken in designing the blocking oscillator is to determine what turns ratio should be used. However, the turns ratio affects a number of things, such as the location of operating points, natural pulse width, etc. in the circuit, so that no single criterion is sufficient to determine n. The range of values imposed upon n by the various requirements in the circuit must be determined first, then a turns ratio can be chosen compatible with all these requirements:

i. The first of these requirements comes from the fact that the turns ratio must be such that the load line intersects the $I(i_b)$ curve in three points. This restricts n to values:

$$n < \frac{I_{cs}}{I_{bs\ \min} - I_{bc}} \doteq \frac{I_{cs}}{I_{bs\ \min}} = \frac{14.5}{2} = 7.25, \tag{81}$$

where $I_{bs\ \min}$ is the minimum base current that will saturate the transistor.

ii. The second requirement pertains to the desirability that n is such that the magnetizing inductance does not significantly affect the location of the quasistable operating point. According to inequality (27), this requires that:

$$n^2 - \frac{I_{cs}}{\dfrac{V_{bs} - E_{bb}}{R_b}} n + \frac{R_b}{L_m}\left(\frac{1}{\omega_0} + R_c C_0\right) \ll 0. \tag{82}$$

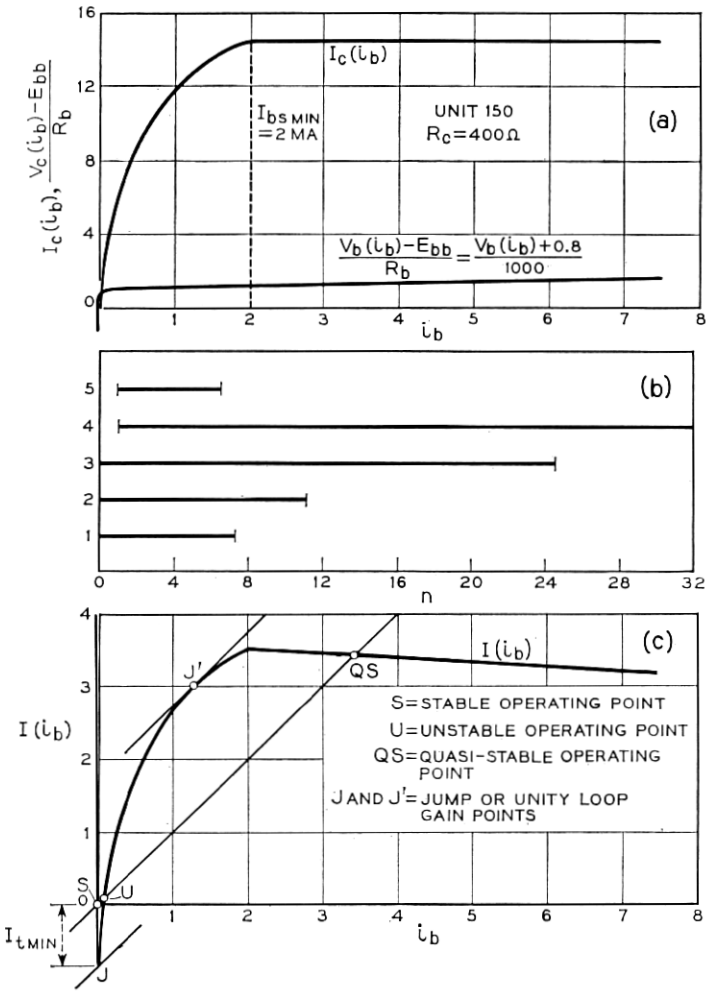

Fig. 27 — Design example: (a) $[V_b(i_b) - E_{bb}]/R_b$ and $I_c(i_b)$ characteristics of 2N128 transistor; (b) range of values imposed upon n; (c) $I(i_b)$ for $n = 3$.

Substituting for ω_0 and C_0 from (28) and (15), respectively, this condition may also be written in the form:

$$n^2 - R_b\left[\frac{I_{cs}}{V_{bs} - E_{bb}} - \frac{1}{L_m}\left(\frac{1}{\omega_\alpha} + 1.5R_cC_c\right)\right]n + \frac{R_b}{L_m}\left[\frac{1}{\omega_\alpha} + R_c(C_s + 1.5C_c)\right] \ll 0. \tag{83}$$

However, in most cases of practical interest,

$$\frac{1}{L_m}\left[\frac{1}{\omega_\alpha} + R_c(C_s + 1.5C_c)\right] \ll \frac{I_{cs}}{V_{bs} - E_{bb}}. \tag{84}$$

Thus, inequality (83) reduces to

$$0 < n < \frac{I_{cs}}{\frac{V_{bs} - E_{bb}}{R_b}}. \tag{85}$$

In our numerical example, condition (84) leads to $5.9 \times 10^{-3} \ll 1.11$. So as far as this requirement is concerned, n should be selected within the range:

$$0 < n < 11.1. \tag{86}$$

iii. In order to assure that the rise time is reasonably independent of $\beta_{\max}$ of the transistor, n should, according to Fig. 13, be selected such that $\beta_{\max}/n$ is not too close to unity, say,

$$n < \frac{\beta_{\max}}{1.5} = \frac{37}{1.5} = 24.6. \tag{87}$$

iv. The fourth requirement on n concerns itself with the desirability of a non-oscillatory recovery, which, according to (77), requires that:

$$n > \sqrt{\frac{2R_b}{\sqrt{\frac{L_m}{C_c + C_s + C_t}}}} = \sqrt{\frac{2 \times 10^3}{\sqrt{\frac{10^{-4}}{3 \times 10^{-11}}}}} = 1.05. \tag{88}$$

v. Finally, in the section on the multipulse response of the blocking oscillator it was found that the natural width should be equal to or larger than three times the time interval, T_T, between the "Turn On" and "Turn Off" pulses in order for the circuit to reproduce the incoming information faithfully. According to (80), this requires that n must be such that:

$$\frac{n^2 L_m}{r_{bs}} \ln \frac{\frac{1}{n} - \frac{E_{bb}}{I_{cs} r_{bs}}}{\frac{I_{bj}}{I_{cs}} - \frac{E_{bb}}{I_{cs} r_{bs}}} \geqq 3T_T. \tag{89}$$

From Figs. 20 or 21 it is seen that this condition will limit n to a range of values between a minimum and a maximum. All quantities are known in the above equation except I_{bj}, which, if n was known, could be determined from Fig. 27(a). However, since the lower and upper limit of n

defined by the above condition approach each other when I_{bj} is increased, and since I_{bj} increases as n is decreased, we only have to consider the case where I_{bj} is determined by the lowest possible value of n. Examining the previous restrictions on n, we see that its smallest possible value is 1.05, which determines the point of tangency in Fig. 27(a) to be $I_{bj} = 2$. Hence, condition (89) becomes

$$n^2 \ln \frac{\frac{1}{n} + 1}{1.138} \geqq 0.564, \tag{90}$$

which gives:

$$0.996 < n < 6.53. \tag{91}$$

The range of values imposed upon n by the above requirements is plotted in Fig. 27(b). It is seen that any value of n between 1.05 and 6.53 satisfies all these requirements. However, remembering that the turns ratio should be selected small in order to reduce the rise time as much as possible, and taking into account that, for reasons of reliability, n should not be chosen close to the edges of the allowable range, the value $n = 3$, seems to be a good compromise. With this value of n the resulting $I(i_b)$ curve is as shown in Fig. 27(c), from which it is seen that the base current at the quasistable operating point is $I_{bs} = 3.42$ ma. Hence, the various circuit parameters become:

$$\omega_0 \sim \frac{\omega_\alpha}{1 + \frac{I_{cs}}{I_{bs}}} = \frac{2\pi 6.08 \times 10^7}{1 + \frac{14.5}{3.42}} = 7.3 \times 10^7, \tag{92}$$

$$C_0 \sim C_s + 1.5C_c\left(1 + \frac{I_{cs}}{I_{bs}}\right) = 5 + 1.5(1.6)\left(1 + \frac{14.5}{3.42}\right) = 17.6\mu\mu\text{f},$$

$$a = \omega_0\sqrt{L_eC_0} = 7.3 \times 10^7\sqrt{10^{-6}(17.8 \times 10^{-12})}$$

$$= 0.31, \tag{93}$$

$$b = \omega_0 R_eC_0 = (7.3 \times 10^7)(1.76 \times 10^{-11}) = 0.52,$$

$$\frac{b}{2a} = 0.84.$$

The normalized trigger pulse width is

$$\tau_w = \omega_0 T_w = (7.3 \times 10^7)(2 \times 10^{-7}) = 14.6. \tag{94}$$

From Fig. 15(c) it is seen that with these values of a and b the normalized rise time is about 4.6, which means that the real rise time is:

$$T_R = \frac{4.6}{7.3 \times 10^7} = 0.063\mu s. \tag{95}$$

Also, from Fig. 16(b) it can be concluded that the overshoot is completely negligible in this case. This is, of course, to be expected, since the ratio $b/2a$ is close to unity.

By separate measurements on the transistor it was determined that the equivalent ω_0 during turnoff was equal to 3×10^7, giving, as before, $a = 0.13$ and $b = 0.21$. According to Fig. 15(c), the fall time is therefore

$$T_F = \frac{3.8}{3.10^7} = 0.127\mu s. \tag{96}$$

Hence, both the rise and fall times are well within the specified limit. If this had not been the case, it would have been necessary to repeat the above procedure with a different trigger source, transformer or load, or with a different transistor.

From Fig. 27(c) it is seen that the minimum trigger magnitude in the case of a very slow trigger is $I_{t\,\min} = 0.85$ and, by interpolation between Figs. 7 and 8, the normalized magnitude for a width of $\tau_w \sim 15$ is $G = 0.175$. Hence, the magnitude of the applied trigger should be larger than:

$$\begin{aligned} I_t &> (I_{bs} - I_{bc})(G - G_{\min}) + I_{t\,\min} \\ &\sim 3.42(0.175 - 0.150) + 0.85 \\ &\sim 0.95 \text{ ma.} \end{aligned} \tag{97}$$

If the blocking oscillator had only been turned "on" externally but left to its own devices afterwards, its natural pulse width would be:

$$T_w = \frac{3^2 \times 10^{-4}}{56.4} \ln \frac{\frac{1}{3} + 1}{\frac{1.25}{14.5} + 1} = 3.35\mu s, \tag{98}$$

where I_{bj} was found from Fig. 27(c) to be equal to 1.25 ma.

The undershoot of the output voltage will be very small since the transformer capacitance is much larger than the output capacitance of the transistor during the recovery interval.

To check how well the above calculations and the rise times predicted by Fig. 15 agreed with experimental results, a blocking oscillator having the same specifications as the one above was built and measured. In the case of the rise times, trigger pulses having magnitudes and widths corresponding exactly to those of Fig. 15 were applied to the circuit and

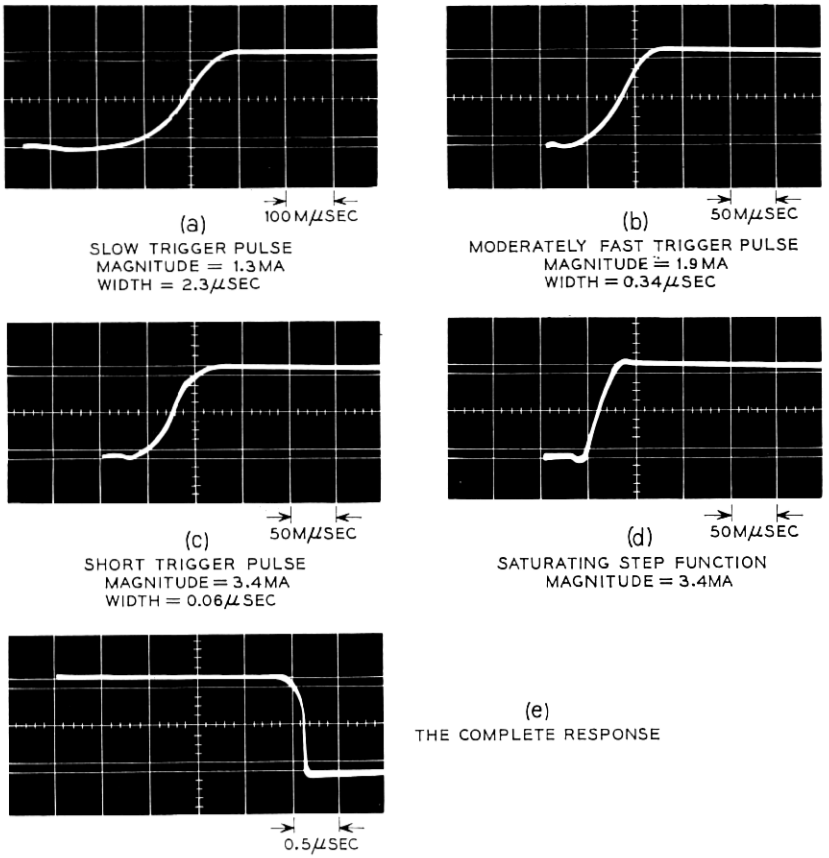

Fig. 28 — (a) through (d) output voltage of the blocking oscillator in response to various types of trigger signals; (e) the complete response.

then compared to the values predicted by these figures. The results are shown in Figs. 28(a) through (d) and in Table III. In all cases the overshoot was not observable, which is what one should expect from Fig. 16. Also, the critical triggering level in the case when a 0.2-microsecond pulse was applied was found to be equal to $I_{t\,\min} = 0.9$ ma. Fig. 28(e) shows the complete response of the blocking oscillator, from which it is seen that its natural pulse width was about 2.5 microseconds and the undershoot less than 5 per cent.

XII. DISCUSSION OF RESULTS

An approach to the design of transistor blocking oscillators with emphasis on the nonlinearities inherent in their operation has been pre-

TABLE III

Trigger Signal	Actual Magnitude, ma	Actual Width, μs	Rise Time, T_R, in μs	
			Calculated	Measured
Slow Trigger Pulse $G = 0.3$, $\tau_w = 166.7$ [Fig. 14(a)]	1.3	2.3	$\frac{11.5}{7.3 \times 10^7} = 0.157$	0.15
Moderately Fast Trigger Pulse $G = 0.5$, $\tau_w = 25$ [Fig. 14(c)]	1.9	0.34	$\frac{4.6}{7.3 \times 10^7} = 0.063$	0.06
Short Trigger Pulse $G = 1$, $\tau_w = 4.175$ [Fig. 14(e)]	3.4	0.06	$\frac{4.65}{7.3 \times 10^7} = 0.064$	0.06
Saturating Step Function $G = 1$ [Fig. 14(f)]	3.4	—	$\frac{2.3}{7.3 \times 10^7} = 0.031$	0.03

sented. A graphical picture of the operating points of the circuit has been drawn which gives a useful feel for the circuit behavior. In addition, both the minimum trigger signal needed to cause the circuit to regenerate, and the requirements for reliable triggering can be inferred from the static characteristic (steady-state equation). An approximate relationship between trigger magnitude and width was determined from analog computations. This relationship, combined with other analysis, shows that the minimum energy for reliable triggering is attained when the transistor has a high-low current β, large ω_α, small collector capacity, and low forward drop (a good switch) and the transformer is of high quality, i.e., has large magnetizing inductance and high coupling coefficients. This is hardly surprising, but it satisfies our intuition. Most importantly, an indication is given as to how these factors affect trigger sensitivity.

The rise time of the circuit is relatively independent of the maximum loop gain $\beta_{\max}/n$, and therefore also of the details of the nonlinear i_c–i_b characteristic for trigger signals about 50 per cent or more larger than the minimum. On the other hand, the rise time is very much dependent upon the rise time of the trigger pulse. Slowly varying triggers give, as expected, the poorest rise time, while the minimum rise time is achieved with fast trigger signals that saturate the transistor immediately. The implications of this result are obvious: power gain and considerable pulse reshaping, as required in a regenerative repeater for PCM, can be purchased at the expense of a rise time significantly slower than that attainable with a sharp trigger signal. This follows from the fact that the positive feedback loop, which is active over a greater portion of the transition on interval with slow trigger signals, has a deleterious effect on rise time. The results of the rise time calculations and the conditions for

monotonic response permit the designer to establish specifications on the circuit to obtain the desired leading edge of the output pulse with small overshoot. The analysis of the "On" interval shows clearly the instabilities in pulse width that result when this width is determined by the natural pulse width of the circuit. It can be seen from Figs. 20 and 21 that the natural pulse width is critically dependent upon the circuit operating points, the nonlinearities and the bias. This is further emphasized by the fact that the largest discrepancy between measured and computed results in the example occurs in the natural pulse width. When the pulse width must be accurately controlled, it is highly desirable to have this accomplished by an external trigger-off pulse. This implies a large magnetizing inductance for the feedback transformer and justifies the initial approximations that were made in the derivation of the equation governing the transition on interval.

During recovery the energy stored in the magnetizing inductance rings out. Quick recovery can be accomplished without retriggering if the transformer circuit is critically damped. This may be accomplished with the existing circuit elements, or it may be necessary to add a damping resistor and diode combination across the transformer.[4] This has the effect of modifying the value of R_b used in the recovery interval. When the circuit is clocked off, analog computer results show that the natural pulse width should be at least three times the desired pulse width for reliable performance.

Several points regarding this analysis and its application should be clarified before concluding. As pointed out, the equivalent circuit chosen for the transistor is a necessity for a tractable analysis. Gross deviations from the assumed configuration may partially invalidate some of the results. In most cases, physical reasoning can be used to account for the effects of these deviations. Furthermore, this equivalent circuit is a good one for transistor designs to shoot for.

Second, the design example clearly shows that the analysis presented does not lead to a set of design equations that can be solved immediately for the values of all the circuit elements. In particular, the parameter n, the turns ratio, is woven into all of the normalized design parameters, as evidenced by the design example. Furthermore, both the magnetizing inductance of the transformer and its parasitic capacity are dependent on n. The fact that there is no simple, immediate means of arriving at a unique set of parameters is due to this interdependence. This is typical of most engineering problems. However, this analysis does bring out the compromises required in the design.

Finally, we believe that the ingredients employed in the present ap-

proach are useful in the successful execution of nonlinear circuit design. The recipe is as follows: apply some experiment; some intuition; some analysis, including minor deviations from superposition, and, finally, a healthy sprinkling of planned computing.

XIII. ACKNOWLEDGMENTS

During the development of this approach to the design of transistor blocking oscillators several stimulating discussions were held with the authors' colleagues. In particular, discussions with F. T. Andrews and R. C. Chapman were most helpful in clarifying some of our concepts. The extensive use of both analog and digital computers is a tribute to the skill and speed with which Mrs. W. L. Mammel, Mrs. G. J. Hansen and Miss E. G. Cheatham coded the problems and nursed them through the computers. S. H. Rothrock made the measurements of the transistor parameters.

APPENDIX A

Derivation of the Differential Equation

From the equivalent circuit in Fig. 2(b) the equations governing blocking oscillator behavior are:

$$i_t = I_t(t), \tag{99}$$

$$v_b = V_b(i_b), \tag{100}$$

$$\left(1 + \frac{1}{\omega_0}\frac{d}{dt}\right) i_c = I_c(ib), \tag{101}$$

$$i_p = ni_s = n\left(i_b + \frac{v_b - E_{bb}}{R_b} - i_t\right), \tag{102}$$

$$i_l = i_p + i_m + i_d = i_p + \frac{1}{L_m}\int_{t_j} \frac{v_b - E_{bb}}{n}\, dt + I_m(t_j) + \frac{C_T}{n}\frac{dv_b}{dt}, \tag{103}$$

$$i_c = i_l - i_g = i_l - C_0\frac{dv_c}{dt}, \tag{104}$$

$$v_c = E_{cc} - i_l R_c - \frac{v_b - E_{bb}}{n} - L_e\frac{di_l}{dt}. \tag{105}$$

Substituting for v_c from (105) in (104):

$$i_c = i_l + C_0 R_c\frac{di_l}{dt} + \frac{C_0}{n}\frac{dv_b}{dt} + L_e C_0\frac{d^2 i_l}{dt^2}, \tag{106}$$

and combining 102 and 103:

$$i_l = ni_b + n\frac{v_b - E_{bb}}{R_b} + \frac{1}{L_m}\int_{t_j}^{t}\frac{v_b - E_{bb}}{n}\,dt + I_m(t_j) + \frac{C_T}{n}\frac{dv_b}{dt} - i_t. \tag{107}$$

Substituting for i_l from (107) into (106) and combining terms yields:

$$\begin{aligned} i_c = {} & L_eC_0n\frac{d^2i_b}{dt^2} + C_0R_cn\frac{di_b}{dt} + ni_b + \frac{L_eC_0C_T}{n}\frac{d^3v_b}{dt^3} \\ & + \frac{L_eC_0n}{R_b} + \frac{C_0C_TR_c}{n}\frac{d^2v_b}{dt^2} + \frac{C_0R_cn}{R_b} + \frac{C_0 + C_T}{n} + \frac{L_eC_0}{L_mn}\frac{dv_b}{dt} \\ & + \frac{n}{R_b} + \frac{C_0R_c}{L_mn}(v_b - E_{bb}) + \frac{1}{L_m}\int_{t_j}^{t}\frac{v_b - E_{bb}}{n}\,dt + I_m(t_j) \\ & - n\left(1 + C_0R_c\frac{d}{dt} + C_0L_e\frac{d^2}{dt^2}\right)i_t. \end{aligned} \tag{108}$$

Operating upon (108) in accordance with (101), grouping like terms, dividing through by n and rewriting in terms of $[v_b(i_b) - E_{bb}]/R_b$ gives the final form of the defining equation as:

$$\begin{aligned} & \frac{L_eC_0}{\omega_0}\frac{d^3i_b}{dt^3} + \left(L_eC_0 + \frac{R_eC_0}{\omega_0}\right)\frac{d^2i_b}{dt^2} + \left(\frac{1}{\omega_0} + R_eC_0\right)\frac{di_b}{dt} \\ & - \left[I(i_b) - i_b - \frac{I_m(t_j)}{n}\right] + \frac{R_b}{n^2L_m}\int_{t_j}^{t}\frac{V_b(i_b) - E_{bb}}{R_b}\,dt \\ & + \left\{\frac{C_TR_b}{n^2} + \frac{1}{\omega_0} + C_0\left[R_e\left(1 + \frac{R_b}{\omega_0n^2L_m}\right) + \frac{R_b}{n^2}\left(1 + \frac{L_e}{L_m}\right)\right]\right\} \\ & \cdot \frac{d}{dt}\frac{V_b(i_b) - E_{bb}}{R_b} + \left\{\frac{C_0C_TR_eR_b}{n^2} + \frac{R_bC_T}{n^2\omega_0} + L_eC_0\right. \\ & \left. + \frac{C_0}{\omega_0}\left[R_e + \frac{R_b}{n^2}\left(1 + \frac{L_e}{L_m}\right)\right]\right\}\frac{d^2}{dt^2}\frac{V_b(i_b) - E_{bb}}{R_b} \\ & + \left(\frac{C_0C_TR_eR_b}{n^2\omega_0} + \frac{L_eC_0}{\omega_0} + \frac{L_eC_0C_TR_b}{n^2}\right)\frac{d^3}{dt^3}\frac{V_b(i_b) - E_{bb}}{R_b} \\ & + \frac{L_eC_0C_TR_b}{n^2\omega^0}\frac{d^4}{dt^4}\frac{V_b(i_b) - E_{bb}}{R_b} \\ & = \left[1 + \left(\frac{1}{\omega_0} + R_eC_0\right)\frac{d}{dt} + \left(L_eC_0 + \frac{R_eC_0}{\omega_0}\right)\frac{d^2}{dt^2} + \frac{L_eC_0}{\omega_0}\frac{d^3}{dt^3}\right]I_t(t). \end{aligned} \tag{109}$$

In the above, $I(i_b)$ is defined as

$$I(i_b) = \frac{I_c(i_b)}{n}\left[1 + \frac{R_b}{n^2L_m}\left(\frac{1}{\omega_0} + R_eC_0\right)\right]\frac{V_b(i_b) - E_{bb}}{R_b}. \tag{110}$$

The "steady-state equation" which determines the operating points of the circuit is given by (109) when all derivatives and integrals are zero. It is

$$I(i_b) - i_b - \frac{I_m(t_j)}{n} = 0. \tag{111}$$

From (107), the output voltage becomes:

$$\begin{aligned} v_0 = R_c i_l = nR_c \Bigg[& i_b + \frac{V_b(i_b) - E_{bb}}{R_b} + \frac{R_b}{n^2 L_m} \int_{t_j}^{t} \frac{V_b(i_b) - E_{bb}}{R_b}\, dt \\ & + R_b \frac{C_T}{n^2} \frac{d}{dt} \frac{V_b(i_b) - E_{bb}}{R_b} + \frac{I_m(t_j)}{n} - I_t(t) \Bigg]. \end{aligned} \tag{112}$$

Combining (105) and (112), the collector voltage may be written

$$v_c = E_{cc} = \frac{V_b(i_b) - E_{bb}}{n} - \left(1 + \frac{L_e}{R_c} \frac{d}{dt}\right) v_0. \tag{113}$$

APPENDIX B

Normalization

Considerable simplification and savings in space can be achieved when the dependent and independent variables are normalized in the following manner:

$$\begin{aligned} \tau &= \omega_0 t, \\ x &= \frac{i_b - I_{bc}}{I_{bs} - I_{bc}} = \text{normalized base current}, \\ V(x) &= \frac{V_b(i_b) - E_{bb}}{R_b(I_{bs} - I_{bc})} = \text{normalized base voltage}, \\ g(\tau) &= \frac{I_t(t)}{I_{bs} - I_{bc}} = \text{normalized trigger function}, \\ f(x) &= \frac{I_c(i_b)}{n(I_{bs} - I_{bc})} \\ &= \text{normalized collector current base current function}, \\ m(\tau_j) &= \frac{I_m(t_j) - nI_{bc}}{n(I_{bs} - I_{bc})} = \text{normalized initial current in } L_m, \\ h(x) &= \frac{I(i_b)}{I_{bs} - I_{bc}} = \text{normalized nonlinear characteristics.} \end{aligned} \tag{114}$$

Further, we define

$$\begin{aligned} a^2 &= \omega_0{}^2 L_e C_0, \\ b &= \omega_0 R_c C_0, \\ c &= \omega_0 \frac{n^2 L_m}{R_b}, \\ d &= \frac{\omega_0 R_b C_0}{n^2}\left(1 + \frac{L_e}{L_m}\right), \\ e &= \frac{\omega_0 R_b C_T}{n^2}, \\ k &= \frac{R_b}{n^2 R_c}. \end{aligned} \tag{115}$$

Using the above definitions in (109) through (111) of Appendix A gives the normalized defining equations:

$$\begin{aligned} &a^2 \frac{d^3x}{d\tau^3} + (a^2 + b)\frac{d^2x}{d\tau^2} + (1 + b)\frac{dx}{d\tau} + x + m - h(x) \\ &\quad + \frac{1}{c}\int_{\tau_j}^{\tau} V(x)\, d\tau + \left[1 + b\left(1 + \frac{1}{c}\right) + d + e\right]\frac{dV(x)}{d\tau} \\ &\quad + (a^2 + b + d + e + be)\frac{d^2V(x)}{d\tau^2} \\ &\quad + (a^2 + be + a^2 e)\frac{d^3V(x)}{d\tau^3} + a^2 e \frac{d^4V(x)}{d\tau^4} \\ &\quad = \left[1 + (1 + b)\frac{d}{d\tau} + (a^2 + b)\frac{d^2}{d\tau^2} + a^2\frac{d^3}{d\tau^3}\right] g(\tau) \end{aligned} \tag{116}$$

and

$$h(x) = f(x) - \left(1 + \frac{1 + b}{c}\right) V(x). \tag{117}$$

The normalized "steady-state equation" which determines the operating points of the circuit is given by (22) in Section IV when all derivatives and integrals are zero. It is

$$h(x) - x - m(\tau_j) = f(x) - \left(1 + \frac{1 + b}{c}\right) V(x) - x - m(\tau_j) = 0. \tag{118}$$

In terms of the normalized base current, x, the stable operating point is

now located at $x = 0$ and the quasistable one at $x = 1$, and $f(x)$ attains the same values at these two points.

If the normalized output voltage is defined as

$$y = \frac{v_0}{nR_c(I_{bs} - I_{bc})} = \frac{i_l}{n(I_{bs} - I_{bc})},$$

the normalized version of (112) of Appendix A becomes

$$y = x + V(x) + \frac{1}{c}\int_{\tau_j}^{\tau} V(x)\, d\tau + e\frac{dV(x)}{d\tau} + m(\tau_j) - g(\tau). \quad (119)$$

In a similar way, the normalized collector voltage is defined as

$$z = \frac{E_{cc} - v_c}{nR_c(I_{bs} - I_{bc})},$$

and (113) of Appendix A becomes

$$z = kV(x) + \left(1 + \frac{a^2}{b}\frac{d}{d\tau}\right) y. \quad (120)$$

REFERENCES

1. Tendick, F. H., Jr., Transistor Pulse Regenerative Amplifiers, B.S.T.J., **35,** September 1956, p. 1085.
2. Wrathall, L. R., Transistorized Binary Pulse Regenerators, B.S.T.J., **35,** September 1956, p. 1059.
3. Linvill, J. G. and Mattson, R. N., Junction Transistor Blocking Oscillators, Proc. I.R.E., **43,** November 1955, p. 1632.
4. Bowers, F. K., unpublished manuscript.
5. Senatorov, K. J. and Guzhov, V. P., On the Analysis of Processes in Transistor Blocking Oscillators, Radio. and Elect. (U.S.S.R.), **2,** 1957, p. 1119.
6. Ebers, J. J. and Moll, J. L., Large-Signal Behavior of Junction Transistors, Proc. I.R.E., **42,** December 1954, p. 1761.
7. Easley, J. W., Effect of Collector Capacity on the Transient Response of Function Transistors, I.R.E. Trans., **ED-4,** January 1957, p. 6.
8. Moll, J. L., Large-Signal Transient Response of Junction Transistors, Proc. I.R.E., **42,** December 1953, p. 1773.
9. Bashkow, T. R., Effect of Nonlinear Collector Capacitance on Collector Current Rise Time, I.R.E. Trans., **ED-3,** October 1956, p. 167.
10. Elmore, W. C. and Sands, M., *Electronics, Experimental Techniques,* McGraw-Hill, New York, 1949, p. 136.
11. Mathers, G. W. C., The Synthesis of Lumped Element Circuits for Optimum Transient Response, Stanford Research Lab. of Electronics Report No. 38, Stanford Univ., Palo Alto, Calif.
12. Narud, J. A., Theory of Nonlinear Feedback Systems Having a Multiple Number of First Order Operating Points and Its Application to Milli-Microsecond Techniques, Atomic Energy Commission Report HEPL-34, February 1955.
13. Aaron, M. R. and Segers, R. G., A Necessary and Sufficient Condition for a Bounded Nondecreasing Step Response, I.R.E. Trans., **CT-5,** September 1958, p. 226.
14. Narud, J. A.,The Secondary Emission Pulse Circuit, Its Analysis and Application, Cruft Lab. Tech. Report No. 245, Harvard Univ., Cambridge, Mass., April 5, 1957, p. 6.